Available online at www.sciencedirect.com
ScienceDirect
Journal of Sound and Vibration 302 (2007) 229–259
JOURNAL OF SOUND AND VIBRATION
www.elsevier.com/locate/jsvi

# Damage detection and generalized Fourier coefficients

Antonino Morassi*

*Dipartimento di Georisorse e Territorio, Università degli Studi di Udine, Via Cotonificio 114, 33100 Udine, Italy*

Received 24 June 2006; received in revised form 22 November 2006; accepted 22 November 2006
Available online 16 January 2007

**Abstract**

This paper deals with damage identification in a vibrating beam, either under axial or bending vibration, based on measurement of damage-induced changes in natural frequencies. It is found that frequency shifts contain information on certain generalized Fourier coefficients of the stiffness variation caused by the damage. Under the assumptions that the damaged beam is a perturbation of the undamaged one and the damage belongs to a half of the beam, a reconstruction procedure based on an iterative algorithm is proposed. The theoretical results are confirmed by a comparison with dynamic measurements on steel beams with localized damages.


## 1. Introduction

Dynamic methods are widely used as a diagnostic tool to detect damage in a structure, see, for example, Ref. [1]. In most studies, changes in natural frequencies represent the dynamic data. In fact, frequencies can be measured more easily than can either mode shapes or time responses, and are less affected by experimental errors.

The approach to damage identification based on frequency measurements is usually of variational type, see Ref. [2]. A function which measures the distance between a certain number of experimental and analytical frequency values is minimized via gradient-type methods and, therefore, the stiffness distribution of a chosen reference configuration of the system is iteratively updated, under some a priori assumptions on the coefficients to be identified (symmetry assumptions, lower and upper bounds, etc.). As discussed, for instance, in Refs. [3,4], the choice of using the frequencies only implies various sources of indeterminacy. In fact, it is well known that existence and uniqueness results in the theory of inverse problems in vibration are available for simple systems only and, even in the case rods and beams, their require knowledge of infinite data, see Gladwell [5,6]. Real situations are substantially different. On one hand, one can measure accurately just the eigenfrequencies of the first few modes of a beam. On the other hand, analytical models of vibrating systems based on classical theories offer a good precision for the first few modes only, rapidly losing accuracy for those of higher order. Then, in studying practical cases one has a finite amount of significant data and the presence

*Tel.: +39 0432 558739; fax: +39 0432 558700.
*E-mail address:* antonino.morassi@uniud.it.

0022-460X/$ - see front matter 
doi:10.1016/j.jsv.2006.11.015

of many solutions cannot be excluded. In fact, the objective function may exhibit several minima that correspond to isolated points, or even continuous regions, in the space of the identification parameters.

Despite the indeterminacy of the mathematical formulation of this class of inverse problems and the lack of satisfactory framework of general properties, some encouraging results have been obtained in last 30 years in studying simple structural systems (see, for example, Refs. [7–10]) and even more complicated vibrating structures (see, for instance, Refs. [11–17]). In particular, damage analyses performed on steel beams and frames with single or multiple notches showed that the results of variational-type methods strictly depend on the accuracy of the structural analytical model that one uses for the interpretation of the experiments and on the severity of the damage to be identified, see, for example, Ref. [18]. Basic questions such as how accurate the description of the reference configuration has to be or which a priori hypotheses are needed to avoid the non uniqueness of the diagnostic problem have been rarely discussed from a general point of view and still are partially open.

With a view to these questions, in this paper the damage detection problem in elastic beams is investigated from a different point of view. Under the assumptions that the damaged configuration is a perturbation of the undamaged one and the linear mass density remains unchanged, the frequency shifts caused by the damage are correlated with some generalized Fourier coefficients of the unknown stiffness variation. This set of Fourier coefficients is determined on a suitable family of functions depending on the vibration modes of the undamaged system. When it is a priori known that the damage belongs to a half of the beam, the measurement of first $M$ frequency shifts, roughly speaking, allows for the determination of the first $M$ generalized Fourier coefficients of the stiffness change evaluated on a chosen basis of functions. A numerical procedure based on an iterative algorithm is proposed for solving the diagnostic problem. The idea of connecting the Fourier coefficients of the unknown coefficient with the frequency shifts is more deep and traces back to the fundamental contribution in inverse eigenvalue theory given by Borg [19], see also Hald [20] and Knobel and Lowe [21] for more recent numerical applications. In the context of crack identification in elastic beams, Wu [22] proposes a reconstruction method by eigenvalues shifts based on the determination of generalized Fourier coefficients of the stiffness variation induced by the damage. In particular, Wu [22] considered an initially uniform pinned–pinned beam with a single symmetric crack at mid-span, see also Wu and Fricke [23] for applications in acoustics to the identification of small blockages in a duct by eigenfrequency shifts.

The predictions of the theory and reliability of the proposed diagnostic technique were checked on the basis of results of several dynamic tests performed on free–free cracked steel beams, both under longitudinal and bending vibrations. It is found that the outcome of the damage analysis via Fourier coefficients depends on the accuracy of the analytical model that one uses for identification and on the severity of the damage. The technique provides a satisfactory identification of the damage, both for position and severity, when frequency shifts induced by the damage are bigger than modelling and measurement errors. For these cases, the results of the damage identification obtained via Fourier coefficient method have been compared with those obtained via a standard variational method based on frequency data. In all the cases considered, the comparison shows a good agreement. This leads to the conjecture that, at least for damage detection in simple beam models, updating the stiffness coefficient of the beam so that the distance between the first $M$ measured and analytical frequencies is minimized, is equivalent to finding the first $M$ generalized Fourier coefficients of the stiffness variation caused by the damage.

The plan of the paper is as follows. The theoretical basis of the method is presented in Section 2 for a rod in longitudinal vibration. An iterative reconstruction procedure is shown in Section 3. Applications to real experimental data for damage identification in rods with single and multiple cracks are discussed in Section 4. The bending vibration case is studied in Section 5. Finally, Section 6 is devoted to a comparison between the results obtained by the proposed diagnostic method and by a variational-type identification technique.

## 2. The theoretical basis of the method

The theoretical basis of the damage identification method is presented for a straight rod in longitudinal vibration. The bending case will be discussed in Section 5.

### 2.1. Formulation of the eigenvalue problem

It is assumed that the spatial variation of the infinitesimal free vibrations of an undamaged rod of length $\ell$ is governed by the differential equation

$$(a(x)u'(x))' + \lambda\rho(x)u(x) = 0 \quad \text{in } (0,\ell), \tag{1}$$

where $u = u(x)$ is the mode shape and $\sqrt{\lambda}$ is the associated natural frequency. The rod is assumed to have no material damping. The quantities $a(x) = EA(x)$ and $\rho(x)$ denote the axial stiffness and the linear-mass density of the rod. $E$ is the Young's modulus of the material and $A(x)$ the cross-section area of the rod.

This analysis is concerned with rods for which $a = a(x)$ is a uniformly strictly positive and continuously differentiable function of $x$ in $[0,\ell]$, namely

$$a \in C^1([0,\ell]), \quad a(x) \geqslant a_0 > 0 \quad \text{in } [0,\ell], \tag{2}$$

where $a_0$ is a given constant. The function $\rho = \rho(x)$ will be assumed to be a continuous and uniformly strictly positive function of $x$ in $[0,\ell]$, that is

$$\rho \in C^0([0,\ell]), \quad \rho(x) \geqslant \rho_0 > 0 \quad \text{in } [0,\ell], \tag{3}$$

where $\rho_0$ is a given constant. Although the present analysis can be developed for general boundary conditions, to fix the ideas the beam is taken with free ends:

$$a(0)u'(0) = 0 = a(\ell)u'(\ell). \tag{4}$$

It is well known that for coefficients $a$ and $\rho$ satisfying (2), (3), respectively, and for end conditions (4), there is an infinite sequence $\{\lambda_m\}_{m=0}^{\infty}$ of real eigenvalues such that $0 = \lambda_0 < \lambda_1 < \lambda_2 < \ldots$, with $\lim_{m\to\infty} \lambda_m = \infty$, see Ref. [24]. Corresponding to every eigenvalue $\lambda_m$ there exists a single eigenfunction $u_m = u_m(x)$, $m = 0, 1, 2, \ldots$, determined up to a multiplicative constant. In order to select uniquely the eigenfunctions, the following *normalization condition* will be used

$$\int_0^\ell \rho u_m^2 \, \mathrm{d}x = 1, \quad m = 0, 1, 2, \ldots \ . \tag{5}$$

The *fundamental mode* $u_0(x)$ of the free–free rod corresponds to $\lambda_0 = 0$ and $u_0(x) = (\int_0^\ell \rho \, \mathrm{d}x)^{-\frac{1}{2}}$ in $[0,\ell]$.

Suppose that a damage appears on the rod. It is assumed that the presence of the damage can be described within the framework of the classical one-dimensional theory of rods and that it reflects on a reduction of the effective axial stiffness without altering the mass distribution, see, for example, Refs. [25,26]. This assumption is rather common in damage detection studies and, in fact, a careful description of damage would be hardly worth doing, since it would require a detailed knowledge of degradation, which is not always available in advance in inverse analysis. More refined mechanical models of beams with localized damages are presented, for example, in Refs. [27,28]. Therefore, in the present analysis, the axial stiffness of the damaged beam will be assumed as follows:

$$a_\varepsilon(x) = a(x) + b_\varepsilon(x), \tag{6}$$

where the *perturbation* introduced by the damage satisfies the conditions:

(i) (regularity of $b_\varepsilon$)

$$b_\varepsilon \in C^1([0,\ell]); \tag{7}$$

(ii) (uniform lower and upper bound of $a_\varepsilon$) there exists a constant $A_0 > 0$ such that

$$a_0 \leqslant a_\varepsilon(x) \leqslant A_0 \quad \text{in } [0,\ell] \tag{8}$$

and

(iii) (smallness of $b_\varepsilon$)

$$\|b_\varepsilon\|_{L^2} = \varepsilon O(\|a\|_{L^2}), \tag{9}$$

for a real positive number $\varepsilon$, where $|O(\|a\|_{L^2})| < c\|a\|_{L^2}$ and $c$ is a positive constant independent of $\varepsilon$.

In Eq. (9), the symbol $\|f\|_{L^2} \equiv (\int_0^\ell f^2(x)\,\mathrm{d}x)^{\frac{1}{2}}$ denotes the norm of the Lebesgue space $L^2(0,\ell)$ of the square summable real-valued functions $f$ on $(0,\ell)$.

A structural damage introduces a reduction of the axial stiffness of the rod, that is

$$b_\varepsilon(x) \leqslant 0 \qquad \text{in } [0,\ell]. \tag{10}$$

The following analysis, however, holds even for a general perturbation $b_\varepsilon(x)$ which takes positive and negative values in $[0,\ell]$.

Under the assumptions (7)–(9), there is an infinite sequence of eigenpairs $\{(u_{m\varepsilon}(x), \lambda_{m\varepsilon})\}_{m=0}^{\infty}$ for the damaged rod, with $0 = \lambda_{0\varepsilon} < \lambda_{1\varepsilon} < \lambda_{2\varepsilon} < \dots$ and $\lim_{m\to\infty} \lambda_{m\varepsilon} = \infty$. Moreover, under the condition (10), the variational formulation of the eigenvalue problem given, for example, in Ref. [24] shows that eigenvalues of the rod are decreasing functions of $b_\varepsilon$, that is

$$\lambda_{m\varepsilon} < \lambda_m, \qquad m = 1, 2, \dots\ . \tag{11}$$

### 2.2. Eigenfrequency sensitivity to damage

In this section, the damaged rod is assumed to be a perturbation of the undamaged one, that is the number $\varepsilon$ appearing in Eq. (9) is small:

$$\varepsilon \ll 1. \tag{12}$$

The smallness of $b_\varepsilon$ expressed by condition (12) allows to include in the analysis either *small* damages given on *large* portions of the interval $[0,\ell]$ (the so-called *diffuse damage*) or severe damages concentrated in small intervals of $[0,\ell]$ (*localized damages*). For example, the coefficient $b_\varepsilon(x) = -\varepsilon a(x)$ in $[0,\ell]$ belongs to the first class; while $b_\varepsilon(x) = \frac{a}{4}(1 + \cos\frac{\pi(x-\ell/4)}{\varepsilon\ell/4})$ in $[\frac{\ell}{4}(1-\varepsilon), \frac{\ell}{4}(1+\varepsilon)]$, with $\varepsilon < 1/2$ and $b_\varepsilon(x) = 0$ elsewhere in $[0,\ell]$, defines a severe damage localized near the cross-section of abscissa $\ell/4$.

Under assumption (12), an asymptotic eigenvalue expansion formula for $\varepsilon \to 0$ will be derived in the sequel.

Let $(u_m, \lambda_m)$, $m = 0, 1, 2, \dots$, be the $m$th normalized eigenpair of the problem (1), (4) corresponding to the undamaged rod, with $a$, $\rho$ satisfying conditions (2) and (3), respectively. Denote by $(u_{m\varepsilon}, \lambda_{m\varepsilon})$, $m = 0, 1, 2, \dots$, the $m$th normalized eigenpair of the perturbed problem

$$(a_\varepsilon(x)u'_{m\varepsilon}(x))' + \lambda_{m\varepsilon}\rho(x)u_{m\varepsilon}(x) = 0 \quad \text{in } (0,\ell), \tag{13}$$

$$a_\varepsilon(0)u'_{m\varepsilon}(0) = 0 = a_\varepsilon(\ell)u'_{m\varepsilon}(\ell), \tag{14}$$

where $a_\varepsilon$ is defined by Eq. (6) and $b_\varepsilon$ satisfies conditions (7)–(9), for a real positive number $\varepsilon$.

The following asymptotic eigenvalue expansion holds true:

$$\lambda_{m\varepsilon} = \lambda_m + \int_0^\ell b_\varepsilon(x)(u'_m(x))^2\,\mathrm{d}x + r(\varepsilon, m), \quad m = 0, 1, 2, \dots, \tag{15}$$

where

$$\lim_{\varepsilon\to 0} \frac{|r(\varepsilon, m)|}{\|b_\varepsilon\|_{L^2}} = 0. \tag{16}$$

Formulae (15), (16) play an important role in this study and, therefore, a proof of them will be sketched in the remaining of the present section.

The proof is based on two main results. The first one is represented by the following *fundamental identity*: for every $\varepsilon > 0$ and for every integer number $m$, $m = 0, 1, 2, \dots$, one has

$$(\lambda_{m\varepsilon} - \lambda_m) \int_0^\ell \rho(x)u_m(x)u_{m\varepsilon}(x)\,\mathrm{d}x = \int_0^\ell b_\varepsilon(x)u'_m(x)u'_{m\varepsilon}(x)\,\mathrm{d}x. \tag{17}$$

Identity (17) can be obtained by multiplying Eq. (13) (with $(u_\varepsilon, \lambda_\varepsilon)$ replaced by the $m$th eigenpair $(u_{m\varepsilon}, \lambda_{m\varepsilon})$) by $u_m$ and Eq. (1) (with $(u, \lambda)$ replaced by the $m$th eigenpair $(u_m, \lambda_m)$) by $u_{m\varepsilon}$, and integrating by parts.

The second result concerns with the asymptotic behavior of the solutions of the eigenvalue problem (13)–(14) as $\varepsilon \to 0$. Since the fundamental mode is insensitive to changes of the stiffness coefficient, when $m = 0$ condition (15) reduces to the identity $\lambda_{0\varepsilon} = \lambda_0$.

Let $m = 1$. By the variational formulation of the eigenvalue problem (13)–(14), the family $\{\lambda_{1\varepsilon}\}_{\varepsilon>0}$ is bounded from above in $\mathbb{R}$. In fact, by Eq. (8), one has

$$\lambda_{1\varepsilon} = \min_{v\in H^1(0,\ell)\setminus\{0\}} \frac{\int_0^\ell a_\varepsilon v'^2\,\mathrm{d}x}{\int_0^\ell \rho v^2\,\mathrm{d}x} \leqslant A_0 \min_{v\in H^1(0,\ell)\setminus\{0\}} \frac{\int_0^\ell v'^2\,\mathrm{d}x}{\int_0^\ell \rho v^2\,\mathrm{d}x} \leqslant c_1, \tag{18}$$

where $c_1 > 0$ is a positive constant independent of $\varepsilon$. In Eq. (18), $H^1(0,\ell)$ denotes the Hilbert space formed by the measurable functions $f$, $f : (0,\ell) \to \mathbb{R}$, such that both $f$ and its first derivative $f'$ (in the sense of distributions) belong to $L^2(0,\ell)$. The norm of the function $f \in H^1(0,\ell)$ is denoted by $\|f\|_{H^1} \equiv (\|f\|_{L^2}^2 + \|f'\|_{L^2}^2)^{\frac{1}{2}}$.

By Eqs. (8) and (18), the family $\{u'_{1\varepsilon}\}_{\varepsilon>0}$, with $\int_0^\ell \rho u_{1\varepsilon}^2\,\mathrm{d}x = 1$ for every $\varepsilon > 0$, is bounded in $L^2(0,\ell)$, namely

$$\int_0^\ell (u'_{1\varepsilon})^2\,\mathrm{d}x \leqslant \frac{1}{a_0}\int_0^\ell a_\varepsilon (u'_{1\varepsilon})^2\,\mathrm{d}x = \frac{\lambda_{1\varepsilon}}{a_0} \leqslant c_2. \tag{19}$$

Therefore, there exists a subsequence of $\{u_{1\varepsilon}\}_{\varepsilon>0}$ (not re-labelled, for the simplicity of notation) such that

$$u_{1\varepsilon} \to u \quad \text{weakly in } H^1(0,\ell) \text{ as } \varepsilon \to 0 \text{ with } \int_0^\ell \rho u^2\,\mathrm{d}x = 1. \tag{20}$$

A sequence $\{g_n\}_{n\geqslant 1} \subset L^2(0,\ell)$ converges weakly to $g \in L^2(0,\ell)$ as $n \to \infty$ if and only if $\int_0^\ell g_n\varphi \to \int_0^\ell g\varphi$ as $n \to \infty$ for every $\varphi \in L^2(0,\ell)$, see Ref. [29] for further details.

Moreover, the family $\{u'_{1\varepsilon}\}$ is uniformly bounded in the Lebesgue space of real-valued bounded functions $L^\infty(0,\ell) = \{f : (0,\ell) \to \mathbb{R}, f \text{measurable and } \|f\|_{L^\infty} \equiv \sup_{x\in(0,\ell)}|f(x)| < \infty\}$, see Ref. [29]. In fact, the differential equation (13) shows that

$$u'_{1\varepsilon}(x) = -\frac{\lambda_{1\varepsilon}}{a_\varepsilon(x)}\int_0^x \rho(s)u_{1\varepsilon}(s)\,\mathrm{d}s \qquad \text{in } [0,\ell], \tag{21}$$

where the boundary condition (14) at $x = 0$ has been used. By Eqs. (8), (18) and Hölder inequality (see Ref. [29]) one has

$$|u'_{1\varepsilon}(x)| \leqslant \frac{c_3}{a_0}\left(\int_0^\ell \rho\,\mathrm{d}s\right)^{1/2} \quad \text{in } [0,\ell] \tag{22}$$

and, therefore,

$$\|u'_{1\varepsilon}\|_{L^\infty} \leqslant c_4, \tag{23}$$

where $c_4 > 0$ is a constant not depending on $\varepsilon$.

Now, it turns out that $u = u_1$ and $\lim_{\varepsilon\to 0}\lambda_{1\varepsilon} = \lambda_1$. To show this, one can take the limit as $\varepsilon \to 0$ in the weak formulation of the eigenvalue problem (13), (14)

$$\int_0^\ell a_\varepsilon u'_{1\varepsilon} f' = \lambda_{1\varepsilon}\int_0^\ell \rho u_{1\varepsilon} f \quad \forall f \in H^1(0,\ell). \tag{24}$$

The left-hand side of Eq. (24) can be written as

$$\int_0^\ell a_\varepsilon u'_{1\varepsilon} f' = \int_0^\ell b_\varepsilon u'_{1\varepsilon} f' + \int_0^\ell a u'_{1\varepsilon} f'. \tag{25}$$

Since $u'_{1\varepsilon} \to u'$ weakly in $L^2(0,\ell)$ as $\varepsilon \to 0$, the second integral in the right-hand side of Eq. (25) converges to $\int_0^\ell au'f'$ as $\varepsilon \to 0$. By the smallness assumption (9) on $b_\varepsilon$ and by Eq. (23), the first integral converges to zero as $\varepsilon \to 0$:

$$\left|\int_0^\ell b_\varepsilon u'_{1\varepsilon} f'\right| \leqslant c_5\|b_\varepsilon\|_{L^2} \leqslant c_5\varepsilon\|a\|_{L^2}, \tag{26}$$

where $c_5$ is a positive constant independent of $\varepsilon$. Therefore, the pair $(u, \lambda = \lim_{\varepsilon\to 0}\lambda_{1\varepsilon})$ satisfies the problem

$$\int_0^\ell au'f' = \lambda\int_0^\ell \rho uf \quad \forall f \in H^1(0,\ell), \tag{27}$$

that is $u = u_1$ and $\lambda = \lambda_1$, with $\int_0^\ell \rho u_1^2\,\mathrm{d}x = 1$.

The convergence of $u_{1\varepsilon}$ to $u_1$ actually is strong in $H^1(0,\ell)$, that is $\|u_{1\varepsilon} - u_1\|_{H^1} \to 0$ as $\varepsilon \to 0$. In fact, let $u_{1\varepsilon}$ be such that $\int_0^\ell \rho u_{1\varepsilon}^2\,\mathrm{d}x = 1$ for every $\varepsilon > 0$, and compute:

$$\int_0^\ell a(u_1' - u_{1\varepsilon}')^2 = \int_0^\ell a(u_1')^2 + \int_0^\ell au_{1\varepsilon}'(u_{1\varepsilon}' - u_1') - \int_0^\ell au_1'u_{1\varepsilon}'. \tag{28}$$

By Eq. (20), the third integral on the right-hand side of Eq. (28) converges to $\int_0^\ell a(u_1')^2$ as $\varepsilon \to 0$. The second integral can be written as

$$\int_0^\ell au_{1\varepsilon}'(u_{1\varepsilon}' - u_1') = \int_0^\ell a_\varepsilon u_{1\varepsilon}'(u_{1\varepsilon}' - u_1') - \int_0^\ell b_\varepsilon u_{1\varepsilon}'(u_{1\varepsilon}' - u_1') \equiv I_{1\varepsilon} + I_{2\varepsilon}. \tag{29}$$

By the uniform estimate (23) of $\{u_{1\varepsilon}'\}$, Hölder inequality and the weak convergence of $u_{1\varepsilon}'$ to $u_1'$ in $L^2(0,\ell)$ as $\varepsilon \to 0$, one has

$$|I_{2\varepsilon}| \leqslant c_6\|u_{1\varepsilon}'\|_{L^\infty}\|b_\varepsilon\|_{L^2}\left(\|u_{1\varepsilon}'\|_{L^2} + \|u_1'\|_{L^2}\right) \leqslant c_7\varepsilon \tag{30}$$

as $\varepsilon \to 0$, where $c_7$ is a positive constant independent of $\varepsilon$.

Concerning the term $I_{1\varepsilon}$, by using the differential equation (13) one has

$$a_\varepsilon(x)u_{1\varepsilon}'(x) = -\lambda_{1\varepsilon}\int_0^x \rho(s)u_{1\varepsilon}(s)\,\mathrm{d}s \quad \text{in } [0,\ell]. \tag{31}$$

Since $\lim_{\varepsilon\to 0}\lambda_{1\varepsilon} = \lambda_1$ and $\lim_{\varepsilon\to 0}\|u_{1\varepsilon} - u_1\|_{L^2} = 0$, one has

$$a_\varepsilon(x)u_{1\varepsilon}'(x) \to -\lambda_1\int_0^x \rho(s)u_1(s)\,\mathrm{d}s \quad \text{strongly in } L^2(0,\ell) \text{ as } \varepsilon \to 0. \tag{32}$$

Therefore, by Eq. (32) and recalling that $u_{1\varepsilon}' \to u'$ weakly in $L^2(0,\ell)$, one has

$$\lim_{\varepsilon\to 0} I_{1\varepsilon} = 0 \tag{33}$$

and this implies that $u_{1\varepsilon} \to u_1$ strongly in $H^1(0,\ell)$ as $\varepsilon \to 0$, with $\int_0^\ell \rho u_1^2\,\mathrm{d}x = 1$.

To obtain the desired eigenvalue expansion (15) for $m = 1$ one can rewrite identity (17) as follows:

$$(\lambda_{1\varepsilon} - \lambda_1)\left(\int_0^\ell \rho u_1^2\,\mathrm{d}x + \int_0^\ell \rho u_1(u_{1\varepsilon} - u_1)\,\mathrm{d}x\right) = \int_0^\ell b_\varepsilon u_1'^2 + \int_0^\ell b_\varepsilon u_1'(u_{1\varepsilon}' - u_1'). \tag{34}$$

Therefore, by the strong convergence in $H^1(0,\ell)$ of $u_{1\varepsilon}$ to $u_1$ as $\varepsilon \to 0$, one has

$$\lambda_{1\varepsilon} - \lambda_1 = \int_0^\ell b_\varepsilon u_1'^2 + o(\|b_\varepsilon\|_{L^2}), \tag{35}$$

where $o(\|b_\varepsilon\|_{L^2})$ is an higher-order term such that $\lim_{\varepsilon\to 0}\frac{o(\|b_\varepsilon\|_{L^2})}{\|b_\varepsilon\|_{L^2}} = 0$.

The proof of Eq. (15) for $m \geqslant 2$ follows the same lines of the case $m = 1$ and it will not repeated here. It is sufficient to recall that the variational formulation of the $m$th eigenvalue problem (13)–(14) includes also the presence of $m - 1$ linear orthogonality constraints, see Ref. [24]. For example, when $m = 2$ one has

$$\lambda_{2\varepsilon} = \min_{v\in H^1(0,\ell)\setminus\{0\},\int_0^\ell \rho v u_{1\varepsilon} = 0} \frac{\int_0^\ell a_\varepsilon v'^2\,\mathrm{d}x}{\int_0^\ell \rho v^2\,\mathrm{d}x}. \tag{36}$$

The limit behavior of the above orthogonality constraint can be easily handled since it is known from the previous case $m = 1$ that $u_{1\varepsilon} \to u_1$ strongly in $L^2(0,\ell)$ as $\varepsilon \to 0$. More generally, in discussing the asymptotic behavior of $\lambda_{m\varepsilon}$, one takes advantage of knowing that $u_{i\varepsilon} \to u_i$ strongly in $L^2(0,\ell)$ as $\varepsilon \to 0$ for every $i$, $i = 1,\ldots,m-1$.

In conclusion, one can notice that Eq. (15) can be read as a series Taylor expansion of the $m$th eigenvalue in terms of the variation $b_\varepsilon$. In fact, in an abstract context, the integral term in Eq. (15) is the *partial derivative* of $\lambda_{m\varepsilon}$ with respect to the axial stiffness coefficient $a_\varepsilon$ evaluated, at $\varepsilon = 0$, on the *direction* $b_\varepsilon$. This partial derivative can be interpreted as the scalar product (in $L^2$-sense) between the *gradient* $\frac{\partial\lambda_{m\varepsilon}}{\partial a_\varepsilon(x)}|_{\varepsilon=0} = (u'_m(x))^2$ and the direction $b_\varepsilon$, namely

$$\left\langle \left.\frac{\partial\lambda_{m\varepsilon}}{\partial a_\varepsilon(x)}\right|_{\varepsilon=0}, b_\varepsilon \right\rangle = \int_0^\ell b_\varepsilon u'^2_m \,\mathrm{d}x. \tag{37}$$

The expression of the integral term in Eq. (15) shows that the sensitivity of the $m$th eigenvalue to changes of the axial stiffness depends on the square of the first derivative of the corresponding $m$th vibration mode of the unperturbed system. When the perturbation $b_\varepsilon$ is localized in a small interval centered in $x_0$, $x_0 \in (0,\ell)$, formula (15) indicates that the first-order variation of the $m$th eigenvalue depends on the square of the longitudinal strain evaluated at $x_0$, see also Refs. [30,31] for an analogous result in the extreme cases of cracks and notches modelled by translational elastic springs inserted at the damaged cross-sections. The explicit expression of the first derivative of an eigenvalue with respect to cracks or notches has been used in Refs. [32–35] to identify localized damages in rods and beams by minimal frequency measurements. Analogous applications to discrete vibrating systems with a single localized damage are presented in Ref. [36].

The analysis has hitherto been related to rods under axial vibration with free ends. However, it is clear that, under analogous assumptions, the asymptotic eigenvalue expansion formula (15) holds true for rods with different boundary conditions, such as, for example, *supported* ($u(0) = 0 = u(\ell)$) or *cantilever* ($u(0) = 0$, $a(\ell)u'(\ell) = 0$).

## 3. A reconstruction procedure

### 3.1. The linearized problem

Let the free vibrations of the reference rod and the perturbed rod be governed by the eigenvalue problems (1), (4) and (13), (14), respectively. The coefficients $a$ and $\rho$ are assumed to satisfy conditions (2) and (3), respectively. In this section, the inverse problem of determining the perturbation $b_\varepsilon$ of the axial stiffness from measurements of the changes in the first $M$ natural frequencies will be considered. The coefficient $b_\varepsilon$ is assumed to satisfy Eqs. (7)–(9) and, in addition, the a priori information

$$\operatorname{supp} b_\varepsilon(x) \equiv \overline{\{x \in (0,\ell) \mid b_\varepsilon(x) \neq 0\}} \subset \left(0, \frac{\ell}{2}\right). \tag{38}$$

The above condition plays an important role in the present study. It should be noticed that there are situations important for applications in which Eq. (38) appears as a rather natural assumption. For example, if the reference beam is symmetrical with respect to $x = \ell/2$, then the eigenvalues $\lambda_{m\varepsilon}(b_{1\varepsilon})$, $\lambda_{m\varepsilon}(b_{2\varepsilon})$ corresponding to two perturbations $b_{1\varepsilon}(x)$, $b_{2\varepsilon}(x)$ symmetrical with respect to $x = \ell/2$, e.g. $b_{1\varepsilon}(\ell - x) = b_{2\varepsilon}(x)$ in $[0,\ell]$, and such that $\operatorname{supp} b_{1\varepsilon} \subset (0,\ell/2)$, $\operatorname{supp} b_{2\varepsilon} \subset (\ell/2,\ell)$, are exactly the same for every $m = 1,2,\ldots$ . Loosely speaking, one can say that the Neumann spectrum cannot distinguish left from the right. To avoid the indeterminacy due to the structural symmetry, condition (38) will be assumed to hold. In practical diagnostic applications, Eq. (38) is equivalent to a priori know that the damage is located on an half of the rod, see, for example, Refs. [3,4] for applications via variational methods. It should be mentioned that diagnostic techniques based on mode shape measurements (see Refs. [37–39]), node measurements (Refs. [40,41]), simultaneous use of resonance and antiresonances (Ref. [42]) have been recently proposed in the specialized literature to avoid the non-uniqueness of the damage location problem in symmetric beam structures.

In order to illustrate the reconstruction procedure, the comparatively simple example of a initially uniform rod, with $a = \text{const.}$ and $\rho = \text{const.}$ in $[0,\ell]$, will be firstly considered. The eigenpairs of the reference rod are given by

$$u_m(x) = \sqrt{\frac{2}{\rho\ell}} \cos\frac{m\pi x}{\ell}, \quad \lambda_m = \frac{a}{\rho}\left(\frac{m\pi}{\ell}\right)^2, \quad m = 1,2,\ldots . \tag{39}$$

The rigid mode $u_0(x)$ is always insensitive to damage and, therefore, it will be omitted in the sequel. Putting the expressions of $\lambda_m$ and $u_m(x)$ for $m \geqslant 1$ into Eq. (15) gives

$$\lambda_{m\varepsilon} - \lambda_m = \left(\frac{m\pi}{\ell}\right)^2 \left(\frac{2}{\rho\ell}\right) \int_0^\ell b_\varepsilon(x) \sin^2 \frac{m\pi x}{\ell}\, \mathrm{d}x + r(\varepsilon, m), \quad m = 1, 2, \ldots, \tag{40}$$

where $r(\varepsilon, m)$ is an higher-order term on $\varepsilon$, see condition (16).

The family $\{\Phi_m(x)\}_{m=1}^\infty$, with $\Phi_m(x) = \frac{(u_m'(x))^2}{\lambda_m} = \frac{2}{a\ell} \sin^2 \frac{m\pi x}{\ell}$ is a basis for the square summable functions defined on $(0, \ell/2)$. This means that any function $f, f : [0, \ell/2] \to \mathbb{R}$ and $f$ regular enough, can be expressed by the series

$$f(x) = \sum_{m=1}^\infty f_m \Phi_m(x), \tag{41}$$

where $f_m$ is the $m$th *generalized Fourier coefficient* of $f$ evaluated on the family $\{\Phi_m(x)\}_{m=1}^\infty$.

By neglecting, as a first approximation, the higher-order term $r(\varepsilon, m)$ in the asymptotic development of the $m$th eigenvalue and expressing $b_\varepsilon$ in terms of the functions $\{\Phi_m(x)\}_{m=1}^\infty$, that is

$$b_\varepsilon(x) = \sum_{k=1}^\infty \beta_{\varepsilon k} \Phi_k(x), \tag{42}$$

one has

$$\delta\lambda_{m\varepsilon} = \sum_{k=1}^\infty A_{mk} \beta_{\varepsilon k}, \quad m = 1, 2, \ldots, \tag{43}$$

where

$$\delta\lambda_{m\varepsilon} \equiv \frac{\lambda_{m\varepsilon} - \lambda_m}{\lambda_m}, \quad m = 1, 2, \ldots, \tag{44}$$

$$A_{mk} \equiv \int_0^{\ell/2} \Phi_m(x) \Phi_k(x)\, \mathrm{d}x = \frac{4}{a^2\ell^2} \int_0^{\ell/2} \sin^2 \frac{m\pi x}{\ell} \sin^2 \frac{k\pi x}{\ell}, \quad k, m = 1, 2, \ldots\ . \tag{45}$$

A direct calculation shows that

$$A_{mk} = \frac{2}{4a^2\ell} \quad \text{for } k \neq m, \quad A_{mk} = \frac{3}{4a^2\ell} \quad \text{for } k = m. \tag{46}$$

In real applications only the eigenvalues of the first few vibrating modes are available. In fact, the number $M$ typically ranges from 3–4 to 10. Therefore, rather than studying the solution of the infinite linear system (43), the following analysis will be focussed on its *M-approximation*, that is the $M \times M$ linear system formed by

$$\delta\lambda_{m\varepsilon} = \sum_{k=1}^M A_{mk}^M \beta_{\varepsilon k}^M, \quad m = 1, \ldots, M, \tag{47}$$

where $A_{mk}^M = A_{mk}$ for $k, m = 1, \ldots, M$, and $\{\beta_{\varepsilon k}^M\}_{k=1}^M$ are the coefficients of the $M$-approximation of $b_\varepsilon(x)$ evaluated on the family $\{\Phi_m(x)\}_{m=1}^\infty$.

A direct calculation shows that

$$\det A_{mk}^M = (2M + 1) \left(\frac{1}{4a^2\ell}\right)^M, \tag{48}$$

$$(A_{mk}^M)^{-1} = (4a^2\ell) \frac{2M - 1}{2M + 1} \quad \text{if } m = k, \quad (A_{mk}^M)^{-1} = -(4a^2\ell) \frac{2}{2M + 1} \quad \text{if } m \neq k, \tag{49}$$

$m,k=1,\ldots,M$. Therefore, the solution of Eq. (47) has the following explicit expression:

$$\beta_{\varepsilon k}^{M}=4a^{2}\ell\left(\frac{2M-1}{2M+1}\delta\lambda_{k\varepsilon}-\frac{2}{2M+1}\sum_{j=1,j\neq k}^{M}\delta\lambda_{j\varepsilon}\right),\quad k=1,\ldots,M, \tag{50}$$

and, going back to Eq. (42), the first-order stiffness change is given by

$$b_{\varepsilon}(x)=8a\sum_{k=1}^{M}\left(\frac{2M-1}{2M+1}\delta\lambda_{k\varepsilon}-\frac{2}{2M+1}\sum_{j=1,j\neq k}^{M}\delta\lambda_{j\varepsilon}\right)\sin^{2}\frac{k\pi x}{\ell}. \tag{51}$$

Expressions (50), (51) clarify how the relative eigenvalue shifts influence the various Fourier coefficients of the stiffness variation $b_{\varepsilon}(x)$. Assuming that the relative eigenvalue shifts are, in average, all of the same order, it can be deduced from Eq. (50) that for relatively large values of $M$ (starting from $M=3$–4, for example), the $k$th Fourier coefficient $\beta_{\varepsilon k}^{M}$ is mainly influenced by the variation of the corresponding $k$th eigenvalue. In fact, for a given $k$ and, for example, for $M=4$, the coefficient which multiplies $\delta\lambda_{k\varepsilon}$ is equal to 0.78 about, whereas the coefficients of the remaining eigenvalue changes $\delta\lambda_{j}$, $j\neq k$, take the lower value 0.22. This difference becomes significant as $M$ increases.

### 3.2. An iterative procedure and a numerical algorithm

The above analysis is based on a linearization of the Taylor series expansion (40) for the eigenvalues of the perturbed rod. Therefore, the coefficient $b_{\varepsilon}$ found by Eq. (51) does not satisfy identically equations (40). The estimation of $b_{\varepsilon}$ can be improved by repeating the procedure shown above starting from the updated configuration $a^{(1)}=a+b_{\varepsilon}$, with $b_{\varepsilon}$ as calculated at the previous step.

This suggests the following iterative procedure for solving the inverse problem. The index $\varepsilon$ has been omitted in this part to simplify the notation. Moreover, $\widetilde{\lambda}_{m}$ denotes the $m$th eigenvalue $\lambda_{m\varepsilon}$ of the perturbed rod.

Iterative procedure and numerical algorithm:

(1) Let $a^{(0)}(x)=a(x)$, where $a(x)$ is the axial stiffness of the reference rod.
(2) For $s=0,1,2,\ldots$:
   (a) solve the linear system

$$\widetilde{\lambda}_{m}-\lambda_{m}^{(s)}=\sum_{k=1}^{M}A_{mk}^{M}\beta_{k}^{M(s)},\quad m=1,\ldots,M, \tag{52}$$

   where $(\lambda_{m}^{(s)},u_{m}^{(s)})$ is the $m$th normalized eigenpair of the problem

$$(a^{(s)}u')'+\lambda^{(s)}\rho u=0\quad\text{in } (0,\ell), \tag{53}$$

$$a^{(s)}(0)u'(0)=0=a^{(s)}(\ell)u'(\ell). \tag{54}$$

   The numbers $\{\beta_{k}^{M(s)}\}_{k=1}^{M}$ are the generalized Fourier coefficients of the unknown function $b^{(s)}(x)$, $b^{(s)}(x)=\sum_{k=1}^{M}\beta_{k}^{M(s)}\Phi_{k}^{(s)}$, and the matrix entries $A_{mk}^{M(s)}$ are given by

$$A_{mk}^{M(s)}=\int_{0}^{\ell/2}\Phi_{m}^{(s)}\Phi_{k}^{(s)}\,\mathrm{d}x,\quad m,k=1,\ldots,M. \tag{55}$$

   (b) Update the coefficient $a(x)$:

$$a^{(s+1)}(x)=a^{(s)}(x)+b^{(s)}(x)\quad\text{in } [0,\ell/2]. \tag{56}$$

(c) If the updated coefficient satisfies the condition

$$\frac{1}{M}\sum_{m=1}^{M}\left(\frac{\widetilde{\lambda}_m-\lambda_m^{(s+1)}}{\widetilde{\lambda}_m}\right)^2<\gamma \tag{57}$$

for a small given control parameter $\gamma$, then stop the iterations. Otherwise, go to step (2) and repeat the procedure.

With the exception of simple cases corresponding to special stiffness coefficients, e.g. $a(x)=\text{const.}$ in $[0,\ell]$, the eigenvalue problem (53)–(54) does not admits closed form eigensolutions. Therefore, for the practical implementation of the identification algorithm resort to numerical analysis in order. The procedure herein adopted is based on a finite element model of the rod with uniform mesh and linear displacement shape functions. The stiffness and mass coefficients are approximated by step functions, that is $a(x)=a_e=\text{const.}$, $\rho(x)=\rho_e=\text{const.}$ within the $e$th finite element. The local mass and stiffness matrices are given by

$$M_e=\rho_e\Delta\begin{pmatrix}\frac{1}{3} & \frac{1}{6}\\ \frac{1}{6} & \frac{1}{3}\end{pmatrix},\quad K_e=a_e\Delta^{-1}\begin{pmatrix}1 & -1\\ -1 & 1\end{pmatrix}, \tag{58}$$

where $\Delta$ is the element length. The discrete approximation of the eigenvalue problem (53)–(54) was solved by the Stodola–Vianello method, see Ref. [43]. The derivative of the eigenfunctions was evaluated by using a finite difference scheme and the numerical integration was developed with a trapezoidal method.

In solving the linear system (52), the determination of the inverse of the matrix $A_{mk}^{M(s)}$ at each step $s$, $s=1,2,\ldots$, is needed. If $s=0$, then $\det A_{mk}^{M(0)}=(2M+1)(4a^2\ell)^{-M}$ by Eq. (48) and the inverse of the matrix $A_{mk}^{M(s)}$ exists. At the first step of the iteration scheme, $s=1$, by Eq. (55) and recalling that

$$u_{m\varepsilon}^{(1)}=u_m^{(0)}+\delta u_{m\varepsilon}, \tag{59}$$

where $\delta u_{m\varepsilon}$ is a *small* perturbation term such that $\|\delta u_{m\varepsilon}\|_{H^1}\to 0$ as $\varepsilon\to 0$, it turns out that

$$A_{mk}^{M(1)}=A_{mk}^{M(0)}+\delta A_{mk,\varepsilon}, \tag{60}$$

where $\delta A_{mk,\varepsilon}\to 0$ as $\varepsilon\to 0$. Therefore, one can conclude that

$$\det A_{mk}^{M(1)}=\det A_{mk}^{M(0)}+\text{ small terms as }\varepsilon\to 0, \tag{61}$$

and the inverse of the matrix $A_{mk}^{M(1)}$ is well defined. By proceeding step by step and within the assumption that the unknown stiffness coefficient is a perturbation of the initial one, the inverse of the matrix $A_{mk}^{M(s)}$ is well defined.

If, during the iterative procedure, the coefficient $a^{(s+1)}$ violates the ellipticity condition (8), then the perturbation $b_\varepsilon^{(s)}$ is multiplied by a suitable step size $\alpha^{(s)}$, typically $\alpha^{(s)}=1/2$, to obtain an updated coefficient satisfying Eq. (8) with $a_0=\frac{1}{100}\min_{x\in[0,\ell]}a^{(0)}(x)$. This procedure is repeated at most five times during each step of the iterative process. After that, the iterations are stopped and the current stiffness distribution is taken as solution of the reconstruction procedure. Analogous considerations hold concerning the upper bound (8) with $A_0=2\max_{x\in[0,\ell]}a^{(0)}(x)$.

The small parameter of the convergence criterion (57) is taken as $\gamma=1.0\times 10^{-12}$ and an upper bound of 50 iterations was introduced.

### 3.3. Some extension

The analysis presented in Sections 3.1, 3.2 is referred to an initially uniform rod under free–free boundary conditions. Aim of this part is to show how the above results can be extended to include rods under different sets of boundary conditions and rods with initial varying profile.

The longitudinal free vibration of an initially uniform rod under supported (S) boundary conditions is firstly considered. Within the notation of the previous sections, the eigenpairs of the unperturbed rod are given by

$$u_m^S(x)=\sqrt{\frac{2}{\rho\ell}}\sin\frac{m\pi x}{\ell},\quad \lambda_m^S=\frac{a}{\rho}\left(\frac{m\pi}{\ell}\right)^2,\quad m=1,2,\ldots\ . \tag{62}$$

Let $\{(u^S_{m\varepsilon}, \lambda^S_{m\varepsilon})\}_{m=1}^{\infty}$ be the (normalized) eigenpairs of the perturbed problem

$$(a_\varepsilon(x)u^{S\,\prime}_{m\varepsilon}(x))' + \lambda^S_{m\varepsilon}\rho(x)u^S_{m\varepsilon}(x) = 0 \quad \text{in } (0,\ell), \tag{63}$$

$$u^S_{m\varepsilon}(0) = 0 = u^S_{m\varepsilon}(\ell), \tag{64}$$

where $a_\varepsilon$ is defined by Eq. (6) and $b_\varepsilon \equiv a_\varepsilon - a$ satisfies conditions (7)–(9), for a real positive number $\varepsilon$.

Putting the expressions of $\lambda^S_{m\varepsilon}$ and $u^S_{m\varepsilon}$, for $m \geqslant 1$, into Eq. (15) (see the remarks at the end of Section 2.2) gives

$$\lambda^S_{m\varepsilon} - \lambda^S_m = \left(\frac{m\pi}{\ell}\right)^2 \left(\frac{2}{\rho\ell}\right) \int_0^\ell b_\varepsilon(x)\cos^2\frac{m\pi x}{\ell}\,\mathrm{d}x + r(\varepsilon, m), \quad m = 1, 2, \ldots, \tag{65}$$

where $\lim_{\varepsilon\to 0}\frac{|r(\varepsilon,m)|}{\varepsilon} = 0$. Since the family $\{\Phi^S_m(x)\}_{m=1}^{\infty}$, where $\Phi^S_m(x) = \frac{(u^{S\,\prime}_m(x))^2}{\lambda^S_m} = \frac{2}{a\ell}\cos^2\frac{m\pi x}{\ell}$, is complete in $L^2(0,\ell/2)$, one can try to find a first approximation of $b_\varepsilon$ by expressing it as a linear combination of the first $M$ functions $\{\Phi^S_m(x)\}_{m=1}^{M}$, as it was made before. Then, an iterative procedure similar to that shown in Sections 3.1, 3.2 can be used to estimate $b_\varepsilon$ in terms of the first $M$ eigenfrequency changes induced by the damage.

Passing to another set of boundary conditions, the $m$th eigenpair of an initially uniform rod with left supported end and free right end (*cantilever* C) is given by

$$u^C_m(x) = \sqrt{\frac{2}{\rho\ell}}\sin\frac{\pi(1+2m)x}{2\ell}, \quad \lambda^C_m = \frac{a}{\rho}\left(\frac{\pi}{2\ell}(1+2m)\right)^2, \quad m = 0, 1, \ldots\ . \tag{66}$$

The family $\{\Phi^C_m(x)\}_{m=0}^{\infty}$, with $\Phi^C_m(x) = \frac{(u^{C\,\prime}_m(x))^2}{\lambda^C_m} = \frac{2}{a\ell}\cos^2\frac{\pi(1+2m)x}{2\ell}$, is complete in $L^2(0,\ell/2)$ and, again, the procedure can be adapted to estimate $b_\varepsilon$.

As it should be clear from the above analysis, a crucial point of the proposed procedure concerns the completeness of the family of (suitably scaled) first derivatives-squares of the longitudinal vibration modes in $L^2(0,\ell/2)$. This property easily follows from the explicit expression of the eigenpairs available in the case of a uniform rod. In the remaining of the present Section, the general case of varying profile is briefly discussed. To simplify the analysis it is decided to consider the case of a rod with free ends and smooth, uniformly positive coefficients $a$ and $\rho$. The method to be accounted for can be easily extended in such a way as to take general boundary conditions.

It is worth pointing out that if $(u_m(x), \lambda_m)$ is an eigenpair of the eigenvalue problem (1), (4), then $(N_m(x) = a(x)u'_m(x), \lambda_m)$ is an eigenpair of the Dirichlet eigenvalue problem

$$(a^*(x)N'_m(x))' + \lambda_m\rho^*(x)N_m(x) = 0 \quad \text{in } (0,\ell), \tag{67}$$

$$N_m(0) = 0 = N_m(\ell), \tag{68}$$

wherein $a^* = \rho^{-1}$, $\rho^* = a^{-1}$.

Now, by the general result by Borg in Ref. [44], the set $\{N^2_m(x)\}_{m=1}^{\infty}$ is complete in $L^2(0,\ell/2)$ and, recalling that $N_m(x) = a(x)u'_m(x)$, this is enough to prove the desired completeness property in the case of varying coefficient.

## 4. Applications

The reconstruction procedure presented in the previous section has been applied to identify stiffness variations caused by localized damages in longitudinally vibrating beams. The principal results of identification are summarized in the sequel.

The experimental models consisted of bars under free–free boundary conditions. Every specimen was damaged by saw-cutting the transversal cross-section. The width of each notch was approximately equal to 1.5 mm and, because of the small level of the excitation, during the dynamic tests each notch remains always open.

In the first experiment, the steel rod of series *HE*100*B* (rod 1) shown in Fig. 1(a) was considered, see Ref. [45] for more details on dynamic testing. By using an impulsive dynamic technique, the first nine natural

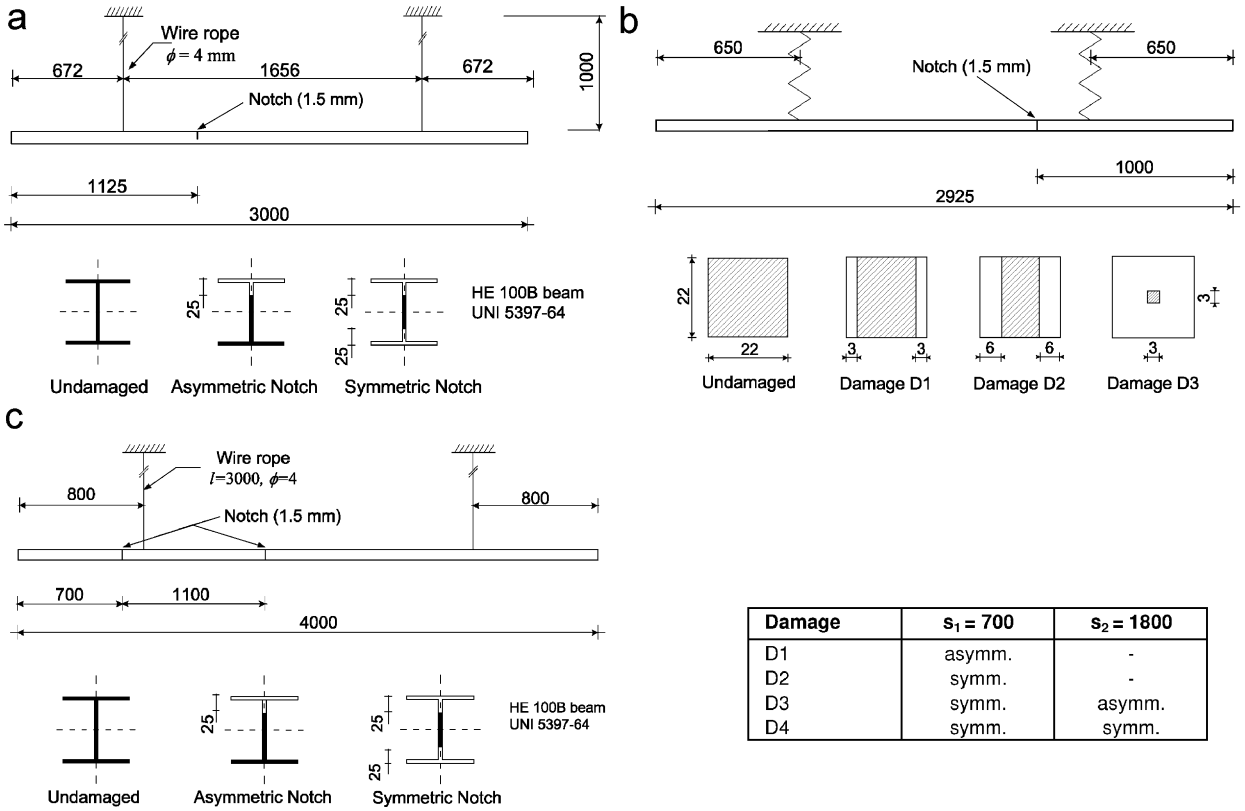


| Damage | $s_1 = 700$ | $s_2 = 1800$ |
|---|---|---|
| D1 | asymm. | - |
| D2 | symm. | - |
| D3 | symm. | asymm. |
| D4 | symm. | symm. |

Fig. 1. (a)–(c) Experimental models of axially vibrating rods and damage configurations: (a) rod 1; (b) rod 2; (c) rod 3. Lengths in mm.

Table 1
Experimental frequencies of rod 1 and analytical values for the undamaged configuration (the rigid body motion is omitted)

| Mode | Undamaged | | | Damage $D1$ | | Damage $D2$ | |
|---|---|---|---|---|---|---|---|
| $n$ | Exper. | Model | $\Delta_n\%$ | Exper. | $\Delta_n\%$ | Exper. | $\Delta_n\%$ |
| 1 | 861.4 | 861.1 | 0.00 | 805.7 | −6.17 | 737.6 | −14.37 |
| 2 | 1722.2 | 1722.2 | 0.00 | 1664.5 | −3.35 | 1600.0 | −7.10 |
| 3 | 2582.9 | 2583.3 | 0.02 | 2541.9 | −1.59 | 2505.3 | −3.00 |
| 4 | 3434.2 | 3444.4 | 0.30 | 3162.2 | −7.92 | 3016.0 | −12.18 |
| 5 | 4353.6 | 4305.5 | −1.10 | 4332.2 | −0.49 | 4310.2 | −1.00 |
| 6 | 5174.4 | 5166.6 | −0.15 | 4961.1 | −4.12 | 4812.6 | −6.99 |
| 7 | 6020.0 | 6027.7 | 0.13 | 5750.2 | −4.48 | 5616.0 | −6.71 |
| 8 | 6870.5 | 6888.8 | 0.27 | 6860.2 | −0.15 | 6851.3 | −0.27 |
| 9 | 7726.4 | 7749.9 | 0.30 | 7302.3 | −5.49 | 7095.8 | −8.16 |

Undamaged configuration: $EA = 5.4454 \times 10^8$ N, $\rho = 20.4$ kg/m, $\ell = 3.0$ m; $\Delta_n\% = 100 \cdot (f_n^{\text{model}} - f_n^{\text{exp}})/f_n^{\text{exp}}$. Damage scenarios $D1$ and $D2$; abscissa of the cracked cross-section $s = 1.125$ m; $\Delta_n\% = 100 \cdot (f_n^{\text{dam}} - f_n^{\text{undam}})/f_n^{\text{undam}}$. Frequency values in Hz.

frequencies of the undamaged bar and of the bar under a series of two damage configurations ($D1$ and $D2$) were determined. The rod was suspended by two steel wire ropes to simulate free–free boundary conditions. The excitation was introduced at one end by means of an impulse force hammer, while the axial response was measured by a piezoelectric accelerometer fixed at the centre of an end cross-section of the rod. Vibration signals were acquired by a dynamic analyzer HP35650 and then determined in the frequency domain to measure the relevant frequency response term (inertance). The well-separated vibration modes and the very

small damping allowed identification of the natural frequencies by means of *single mode technique*. The damage configurations were obtained by introducing a notch of increasing depth at $s = 1.125$ m from one end. Table 1 compares the first nine experimental natural frequencies for the undamaged and damaged rod. The analytical model of the undamaged configuration generally fits well with the real case and the percentage errors are lower than 1% within the measured modes. The eigenfrequency shifts induced by the damage are relatively large with respect to the modelling errors and rod 1 provides an example for which the damage is rather severe from the beginning.

The rod was discretized in 200 equally spaced finite elements and the identification procedure was applied by considering an increasing number of natural frequencies $M$, $M = 1, \ldots, 9$. The chosen finite element mesh guarantees for the presence of negligible discretization errors during the identification process. Figs. 2 and 3 show the identified stiffness coefficient when $M = 3, 5, 7, 9$ natural frequencies are considered in identification, for damage $D1$ and $D2$, respectively. Convergence of the iterative process seems to be rather fast and, typically, less than 10 iterations are sufficient to reach the optimal solution.

As it was expected from the representation formula (42), the reconstruction coefficient shows a wavy behavior around the reference (constant) value $a_0$. The maximum values of the positive increments are, in some cases, comparable with the maximum reduction in stiffness, which occurs near the actual damage location $s = 1.125$ m. However, the extent of the regions with positive change in stiffness becomes less important as the number of frequencies $M$ increases and when more severe levels of damage are considered in the analysis.

From Figs. 2 and 3 it can been seen that the reconstructed coefficient can give an indication where the damage is located. The results of identification can be slightly improved by recalling that, from the physical point of view, the coefficient $a_{\mathrm{dam}}(x)$ clearly cannot be greater than the reference value $a_0(x)$. This suggests to a posteriori set the identified coefficient to be equal to $a^{(0)}(x)$ wherever $a_{\mathrm{dam}}(x) > a^{(0)}(x)$, see also Ref. [22].

The results of most diagnostic techniques based on dynamic data strictly depend on the accuracy of the analytical model considered for the interpretation of the measurements and the severity of the damage to be identified. Rod 1 provides an example for which the analytical model (of the reference system) is very accurate

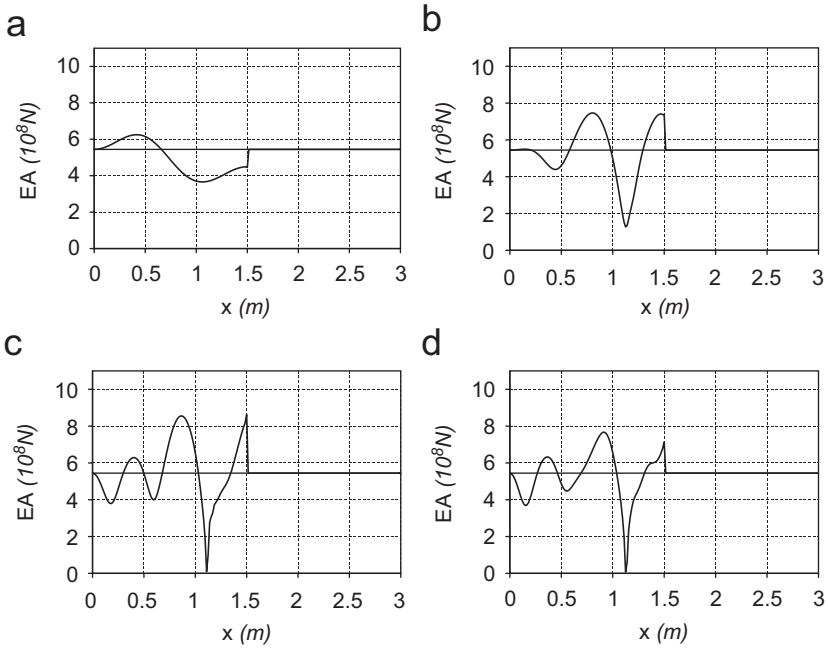


Fig. 2. (a)–(d) Rod 1: identified axial stiffness $EA$ for damage $D1$ with $M = 3$ (a), $M = 5$ (b), $M = 7$ (c) and $M = 9$ (d) frequencies. Actual damage location $s = 1.125$ m.

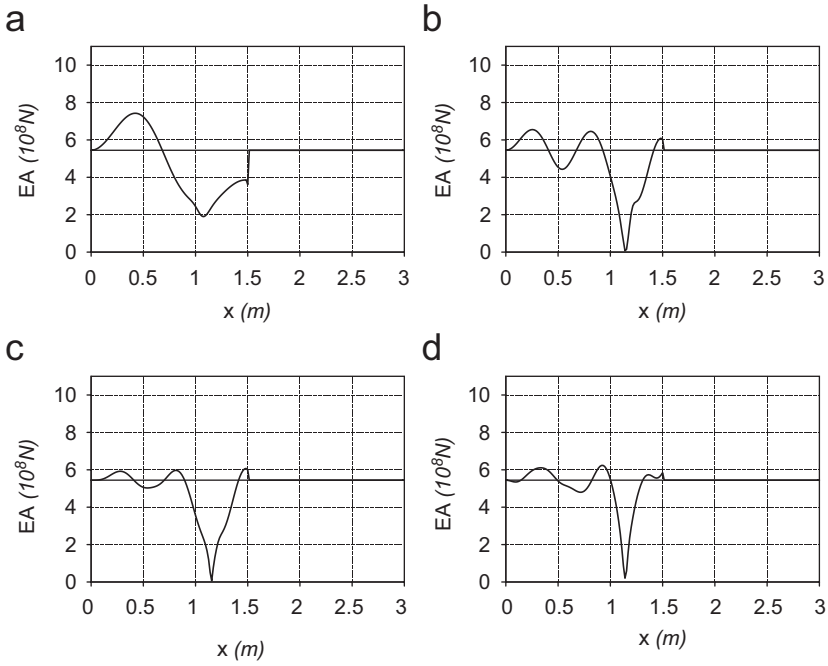


Fig. 3. (a)–(d) Rod 1: identified axial stiffness $EA$ for damage $D2$ with $M = 3$ (a), $M = 5$ (b), $M = 7$ (c) and $M = 9$ (d) frequencies. Actual damage location $s = 1.125$ m.

and for which the damage is rather severe from the beginning. Therefore, in order to study the sensitivity of the proposed reconstruction procedure to small levels of damage, in the second experiment a steel rod of square solid cross-section with a small crack was considered (rod 2). By adopting an experimental technique similar to that used for rod 1, the undamaged bar and three damaged configurations obtained by introducing a notch of increasing depth at $s = 1.000$ m from one end, see Fig. 1(b).

The analytical model turns out to be extremely accurate with percentage errors less than those of the first experiment and lower than 0.2% within the first 20 vibrating modes, cf. Table 2.

The percentage of frequency shifts caused by the damage are of order 0.1% and 0.3–0.4% for damage $D1$ and $D2$, respectively. Therefore, for these two configurations it is expected that modelling errors could mask the changes induced by damage. The results of identification are summed up in Figs. 4–7 for an increasing number of frequencies. It can be seen that a reduction of stiffness near the actual damage location appears for the configuration $D2$ when more than 5 frequencies are considered in identification. Figs. 6 and 7 show that the damage $D3$ is clearly identified when the first 3–5 frequencies are measured. In this case, the results show a good stability of the identification when an increasing number of frequencies is considered in the analysis.

In the third experiment, the diagnostic technique was tested on a free–free longitudinally vibrating beam (rod 3) with multiple localized damages. The experimental model is shown in Fig. 1(c) and Table 3 compares the first nine measured frequencies for four damage configurations $D1$–$D4$. Configurations $D1$ and $D2$ correspond, respectively, to an asymmetric and a symmetric notch of increasing depth placed at the same cross-section of the rod, at 0.700 m from the left end. Configurations $D3$ and $D4$ were obtained in a similar way by saw-cutting the beam at progressive depth at 1.100 m far from the previous notched cross-section. As for rod 1, this experimental model is characterized by damages which are rather severe from the beginning. Eigenfrequency reductions, in fact, are of order 1–5% and 1–12% for first two configurations $D1$ and $D2$, respectively, and they belong to the range 5–20% in the most severe level of damage $D4$. The results of damage identification are summarized in Figs. 8–11 and they essentially confirm those obtained for the previous cases. In particular, the identification method seems to be able to estimate the position of multiple cracks in the rod when at least 5–7 frequencies are considered in the analysis. These results suggest that, when it is a priori

Table 2
Experimental frequencies of rod 2 and analytical values for the undamaged configuration (the rigid body motion is omitted)

| Mode | Undamaged | | | Damage $D1$ | | Damage $D2$ | | Damage $D3$ | |
|---|---|---|---|---|---|---|---|---|---|
| $n$ | Exper. | Model | $\Delta_n\%$ | Exper. | $\Delta_n\%$ | Exper. | $\Delta_n\%$ | Exper. | $\Delta_n\%$ |
| 1 | 882.25 | 882.25 | 0.00 | 881.5 | −0.09 | 879.3 | −0.33 | 831.0 | −5.81 |
| 2 | 1764.6 | 1764.5 | −0.01 | 1763.3 | −0.07 | 1759.0 | −0.32 | 1679.5 | −4.82 |
| 3 | 2645.8 | 2646.8 | 0.04 | 2644.0 | −0.07 | 2647.0 | 0.05 | 2646.5 | 0.03 |
| 4 | 3530.3 | 3529.0 | −0.04 | 3526.8 | −0.10 | 3516.5 | −0.39 | 3306.0 | −6.35 |
| 5 | 4411.9 | 4411.3 | −0.01 | 4408.8 | −0.07 | 4400.0 | −0.27 | 4250.0 | −3.67 |
| 6 | 5293.9 | 5293.5 | −0.01 | 5294.3 | 0.01 | 5295.3 | 0.03 | 5287.8 | −0.12 |
| 7 | 6175.4 | 6175.8 | 0.01 | 6168.8 | −0.11 | 6150.3 | −0.41 | 5808.5 | −5.94 |
| 8 | 7056.7 | 7058.0 | 0.02 | 7052.0 | −0.07 | 7039.5 | −0.24 | 6864.3 | −2.73 |
| 9 | 7937.9 | 7940.3 | 0.03 | 7937.5 | −0.01 | 7938.0 | 0.00 | 7909.5 | −0.36 |
| 10 | 8819.9 | 8822.5 | 0.03 | 8809.8 | −0.11 | 8782.0 | −0.43 | 8340.0 | −5.44 |
| 11 | 9702.7 | 9704.8 | 0.02 | 9697.3 | −0.06 | 9682.8 | −0.21 | 9503.3 | −2.06 |
| 12 | 10583.8 | 10587.0 | 0.03 | 10582.8 | −0.02 | 10581.3 | −0.02 | 10514.8 | −0.65 |
| 13 | 11464.3 | 11469.3 | 0.04 | 11449.0 | −0.13 | 11410.5 | −0.47 | 10933.5 | −4.63 |
| 14 | 12345.2 | 12351.5 | 0.05 | 12339.5 | −0.05 | 12331.5 | −0.11 | 12158.0 | −1.52 |
| 15 | 13224.4 | 13233.8 | 0.07 | 13222.8 | −0.01 | 13322.0 | +0.74 | 13098.0 | −0.96 |
| 16 | 14104.0 | 14116.0 | 0.09 | 14087.0 | −0.12 | 14039.0 | −0.46 | 13543.0 | −3.98 |
| 17 | 14985.0 | 14998.0 | 0.09 | 14979.0 | −0.04 | 14964.0 | −0.14 | 14811.0 | −1.16 |

Undamaged configuration: $EA = 9.9491 \times 10^7$ N, $\rho = 3.735$ kg/m, $\ell = 2.925$ m; $\Delta_n\% = 100 \cdot (f_n^{\text{model}} - f_n^{\text{exp}})/f_n^{\text{exp}}$. Damage scenarios $D1$, $D2$ and $D3$; abscissa of the cracked cross-section $s = 1.000$ m; $\Delta_n\% = 100 \cdot (f_n^{\text{dam}} - f_n^{\text{undam}})/f_n^{\text{undam}}$. Frequency values in Hz.

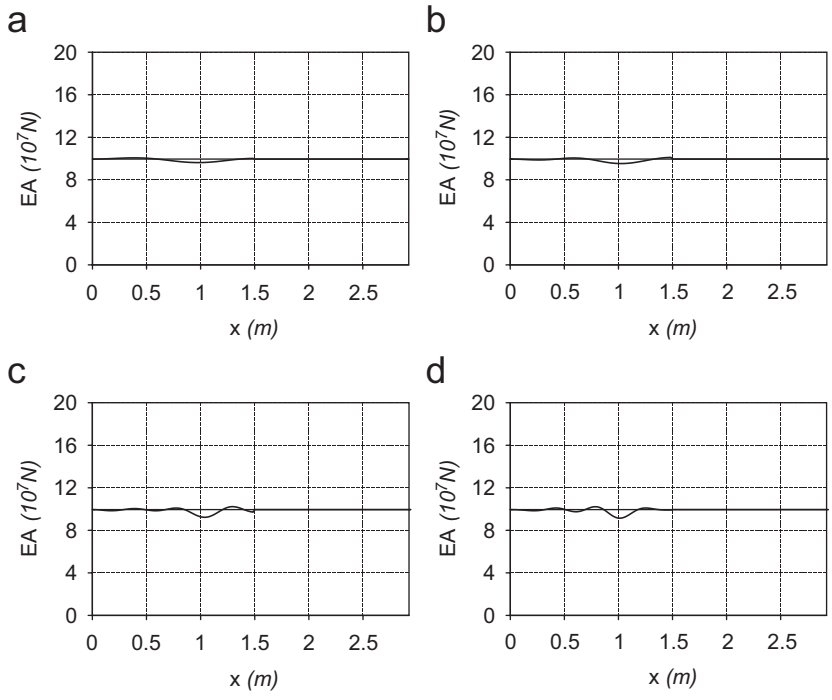


Fig. 4. (a)–(d) Rod 2: identified axial stiffness $EA$ for damage $D2$ with $M = 3$ (a), $M = 5$ (b), $M = 7$ (c) and $M = 9$ (d) frequencies. Actual damage location $s = 1.000$ m.

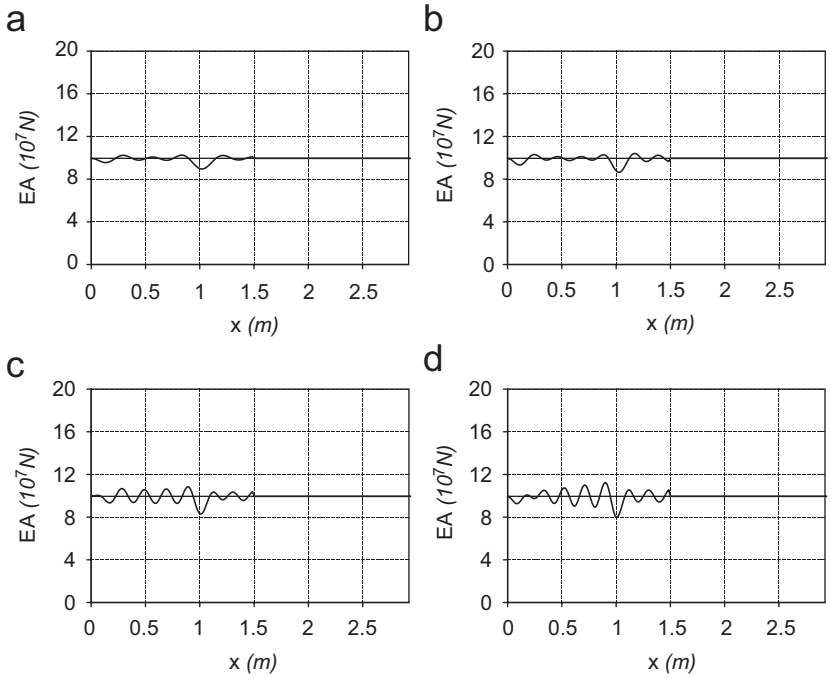


Fig. 5. (a)–(d) Rod 2: identified axial stiffness $EA$ for damage $D2$ with $M = 11$ (a), $M = 13$ (b), $M = 15$ (c) and $M = 17$ (d) frequencies. Actual damage location $s = 1.000$ m.

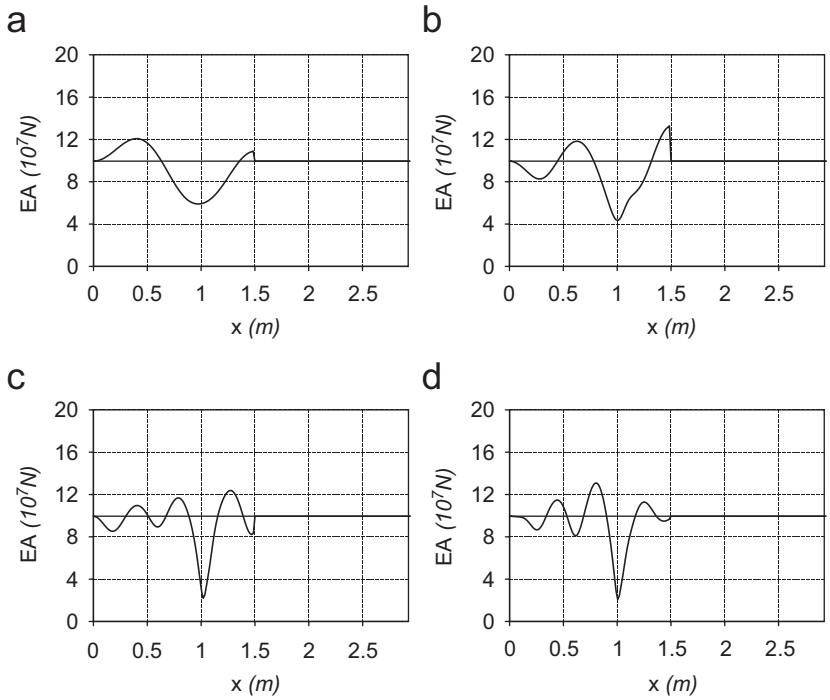


Fig. 6. (a)–(d) Rod 2: identified axial stiffness $EA$ for damage $D3$ with $M = 3$ (a), $M = 5$ (b), $M = 7$ (c) and $M = 9$ (d) frequencies. Actual damage location $s = 1.000$ m.

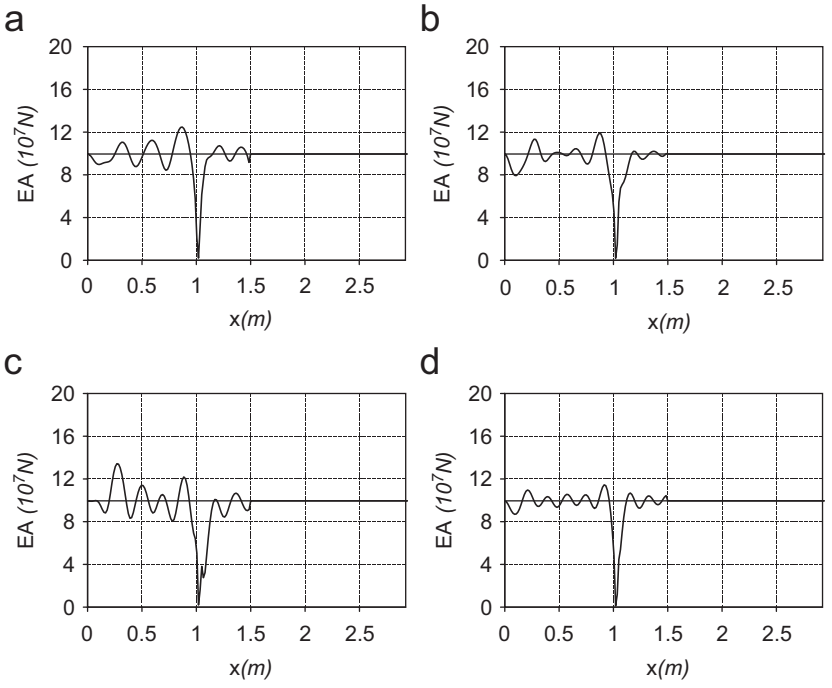


Fig. 7. (a)–(d) Rod 2: identified axial stiffness $EA$ for damage $D3$ with $M = 11$ (a), $M = 13$ (b), $M = 15$ (c) and $M = 17$ (d) frequencies. Actual damage location $s = 1.000$ m.

Table 3
Experimental frequencies of rod 3 and analytical values for the undamaged configuration (the rigid body motion is omitted)

| Mode | Undamaged | | | Damage $D1$ | | Damage $D2$ | | Damage $D3$ | | Damage $D4$ | |
|---|---|---|---|---|---|---|---|---|---|---|---|
| $n$ | Exper. | Model | $\Delta_n$% | Exper. | $\Delta_n$% | Exper. | $\Delta_n$% | Exper. | $\Delta_n$% | Exper. | $\Delta_n$% |
| 1 | 646.13 | 646.13 | 0.00 | 637.0 | −1.41 | 618.5 | −4.28 | 589.3 | −8.8 | 548.9 | −15.1 |
| 2 | 1290.9 | 1292.3 | 0.11 | 1202.4 | −6.86 | 1142.1 | −11.52 | 1142.6 | −11.5 | 1140.8 | −11.6 |
| 3 | 1935.1 | 1938.4 | 0.17 | 1846.0 | −4.61 | 1744.8 | −9.84 | 1651.6 | −14.7 | 1539.3 | −20.5 |
| 4 | 2579.9 | 2584.5 | 0.18 | 2495.5 | −3.27 | 2450.9 | −5.00 | 2438.4 | −5.5 | 2425.5 | −6.0 |
| 5 | 3220.3 | 3230.6 | 0.32 | 3199.6 | −0.64 | 3180.9 | −1.22 | 3072.5 | −4.6 | 2907.0 | −9.7 |
| 6 | 3844.6 | 3876.8 | 0.84 | 3834.0 | −0.28 | 3817.4 | −0.79 | 3757.0 | −2.3 | 3639.0 | −5.4 |
| 7 | 4544.5 | 4522.9 | −0.48 | 4407.4 | −3.02 | 4054.9 | −10.77 | 4000.6 | −12.0 | 3980.9 | −12.4 |
| 8 | 5169.9 | 5169.9 | −0.02 | 4904.5 | −5.13 | 4801.1 | −7.13 | 4782.0 | −7.5 | 4771.8 | −7.7 |
| 9 | 5809.3 | 5815.1 | 0.10 | 5711.4 | −1.68 | 5541.8 | −4.61 | 5262.3 | −9.4 | 5137.6 | −11.6 |

Undamaged configuration: $EA = 5.5508 \times 10^8$ N, $\rho = 20.775$ kg/m, $\ell = 4.000$ m; $\Delta_n\% = 100 \cdot (f_n^{\text{model}} - f_n^{\text{exp}})/f_n^{\text{exp}}$. Damage scenarios $D1$, $D2$, $D3$ and $D4$; abscissa of the cracked cross-sections: $s_1 = 0.700$ m, $s_2 = 1.800$ m; $\Delta_n\% = 100 \cdot (f_n^{\text{dam}} - f_n^{\text{undam}})/f_n^{\text{undam}}$. Frequency values in Hz.

known that the damages are concentrated, the proposed method can be advantageously applied to obtain information on the number of the damages present in the rod.

## 5. The bending vibration case

In the previous sections, the problem of identifying the stiffness change induced by a damage in an axially vibrating beam from frequency measurements has been discussed. Here, the corresponding problem for a beam in bending vibration will be considered.

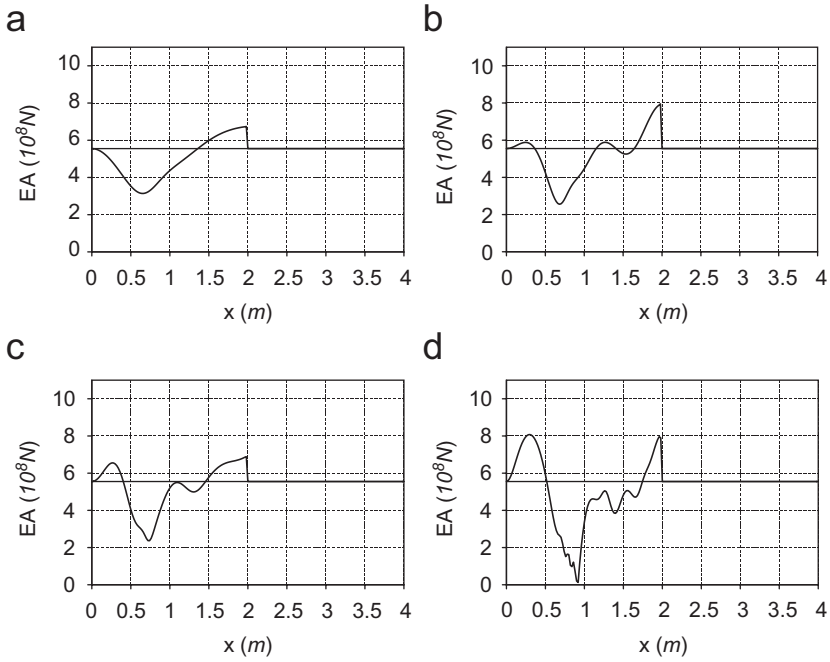


Fig. 8. (a)–(d) Rod 3: identified axial stiffness $EA$ for damage $D1$ with $M = 3$ (a), $M = 5$ (b), $M = 7$ (c) and $M = 9$ (d) frequencies. Actual damage location $s_1 = 0.700$ m.

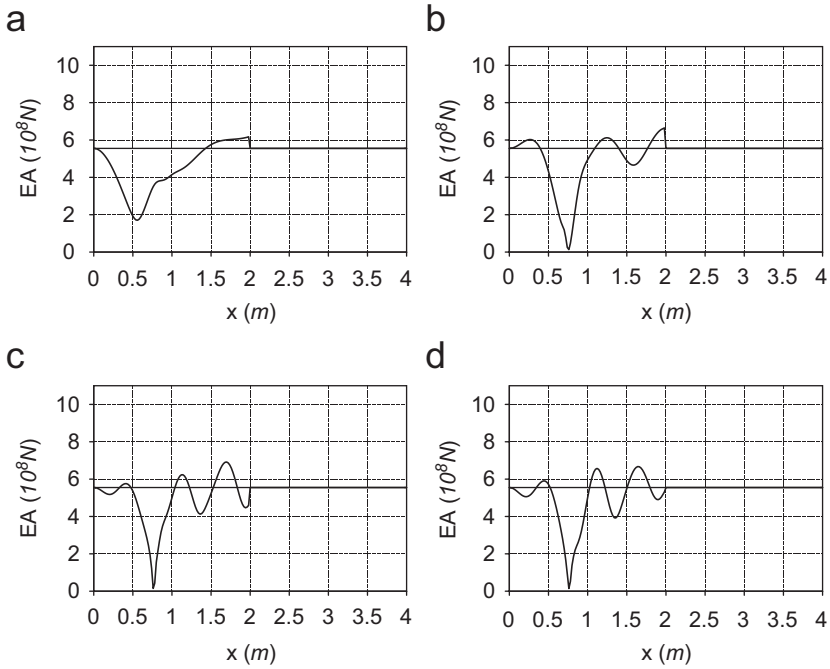


Fig. 9. (a)–(d) Rod 3: identified axial stiffness $EA$ for damage $D2$ with $M = 3$ (a), $M = 5$ (b), $M = 7$ (c) and $M = 9$ (d) frequencies. Actual damage location $s_1 = 0.700$ m.

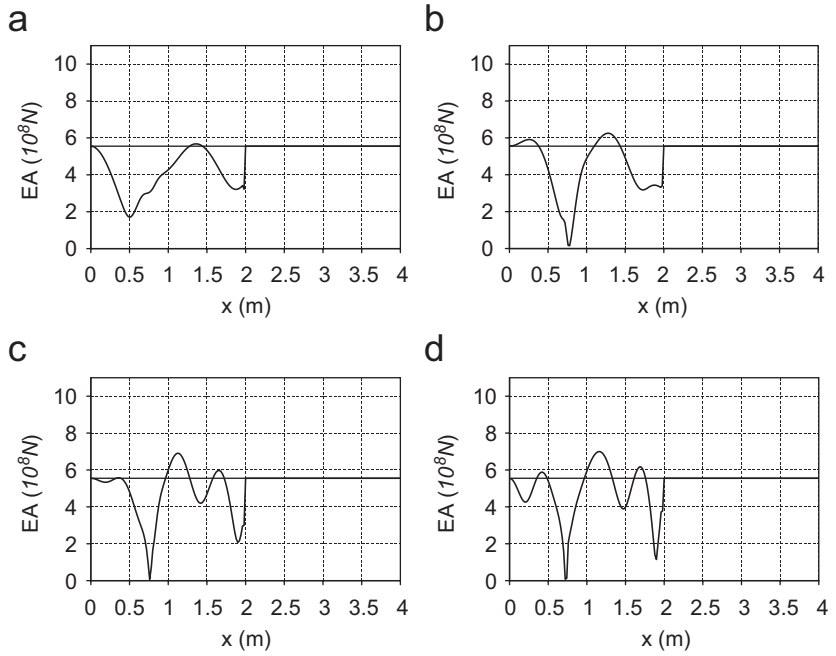


Fig. 10. (a)–(d) Rod 3: identified axial stiffness $EA$ for multiple damage $D3$ with $M = 3$ (a), $M = 5$ (b), $M = 7$ (c) and $M = 9$ (d) frequencies. Actual damage locations $s_1 = 0.700$ m and $s_2 = 1.800$ m.

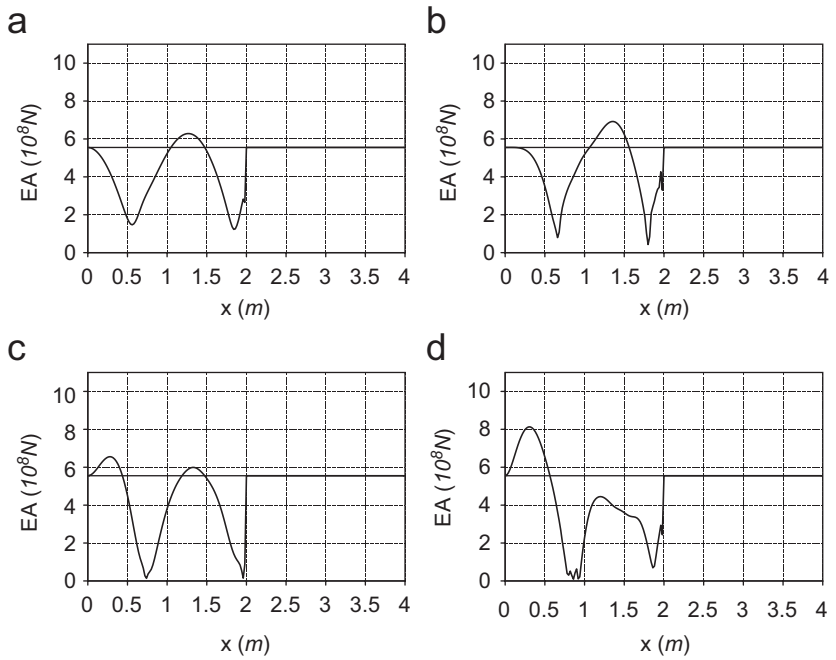


Fig. 11. (a)–(d) Rod 3: identified axial stiffness $EA$ for multiple damage $D4$ with $M = 3$ (a), $M = 5$ (b), $M = 7$ (c) and $M = 9$ (d) frequencies. Actual damage locations $s_1 = 0.700$ m and $s_2 = 1.800$ m.

### 5.1. The reconstruction procedure in the bending case

The physical model, which will be investigate, is a simply supported Euler–Bernoulli beam. The undamped free vibration of the undamaged beam are governed by the boundary-value problem

$$(j(x)v''(x))'' - \lambda\rho(x)v(x) = 0 \quad \text{in } (0,\ell),$$

$$v(0) = 0 = v(\ell),$$

$$j(0)v''(0) = 0 = j(\ell)v''(\ell), \tag{69}$$

where $v = v(x)$ is the transversal displacement of the beam, $\sqrt{\lambda}$ is the associated natural frequency and $\rho = \rho(x)$ denotes the linear mass density. The quantity $j(x) = EJ(x)$ is the bending stiffness of the beam. $E$ is the Young's modulus of the material and $J = J(x)$ the moment of inertia of the cross-section. The function $\rho$ is assumed to satisfy conditions (3). The bending stiffness $j$ is such that

$$j \in C^2([0,\ell]), \quad j(x) \geqslant j_0 > 0 \quad \text{in } [0,\ell], \tag{70}$$

where $j_0$ is a given constant.

Under the above assumptions on the coefficients, problem (69) has an infinite sequence of eigenpairs $\{(v_m, \lambda_m)\}_{m=1}^{\infty}$, with $0 < \lambda_1 < \lambda_2 < \ldots$, $\lim_{m\to\infty} \lambda_m = \infty$ and where the $m$th vibration mode is assumed to satisfy the normalization condition $\int_0^\ell \rho v_m^2 = 1$ for every $m$, $m \geqslant 1$.

In analogy with the axial case, it is assumed that a structural damage can be described within the classical one-dimensional theory of beams and that it reflects on a reduction of the effective bending stiffness, without introducing changes on the mass distribution. Following the analysis presented in Section 2.2, the bending stiffness of the damaged beam is taken as

$$j_\varepsilon(x) = j(x) + b_\varepsilon(x), \tag{71}$$

where the perturbation $b_\varepsilon$ is assumed to satisfy the following conditions:

(i) (regularity of $b_\varepsilon$)

$$b_\varepsilon \in C^2([0,\ell]); \tag{72}$$

(ii) (uniform lower and upper bound of $j_\varepsilon$) there exist a constant $J_0$ such that

$$j_0 \leqslant j_\varepsilon(x) \leqslant J_0 \quad \text{in } [0,\ell]; \tag{73}$$

(iii) (smallness of $j_\varepsilon$)

$$\|b_\varepsilon\|_{L^2} = \varepsilon O(\|j\|_{L^2}) \tag{74}$$

for a real positive number $\varepsilon$.

The free bending vibrations of the damaged beam are governed by the eigenvalue problem

$$(j_\varepsilon v_\varepsilon'')'' - \lambda_\varepsilon \rho v_\varepsilon = 0 \quad \text{in } (0,\ell),$$

$$v_\varepsilon(0) = 0 = v_\varepsilon(\ell),$$

$$j_\varepsilon(0)v_\varepsilon''(0) = 0 = j_\varepsilon(\ell)v_\varepsilon''(\ell). \tag{75}$$

Under the above assumptions (72)–(74), the perturbed problem has a sequence of eigenpairs $\{(v_{m\varepsilon}, \lambda_{m\varepsilon})\}_{m=1}^{\infty}$, with $0 < \lambda_{1\varepsilon} < \lambda_{2\varepsilon} < \ldots$ and $\lim_{m\to\infty} \lambda_{m\varepsilon} = \infty$. The $m$th vibration mode is assumed to satisfy the normalization condition $\int_0^\ell \rho v_{m\varepsilon}^2 = 1$ for every $m$, $m \geqslant 1$, and for every $\varepsilon > 0$.

The present analysis will concern with perturbations of the reference beam. This condition is expressed by requiring that

$$\varepsilon \ll 1. \tag{76}$$

By applying a technique similar to that shown in Section 2.2 for the longitudinal vibration case, the following asymptotic development for the $m$th eigenvalue holds:

$$\lambda_{m\varepsilon} = \lambda_m + \int_0^\ell b_\varepsilon(x)(v_m''(x))^2 \,\mathrm{d}x + r(\varepsilon, m), \quad m = 1, 2, \ldots, \tag{77}$$

where

$$\lim_{\varepsilon \to 0} \frac{|r(\varepsilon, m)|}{\|b_\varepsilon\|_{L^2}} = 0. \tag{78}$$

As in the second-order case, the main point of the proof concerns with the asymptotic behavior of the eigensolutions $\{(v_{m\varepsilon}, \lambda_{m\varepsilon})\}_{m=1}^\infty$ as $\varepsilon \to 0$. On adapting the arguments presented from Eq. (18) to Eq. (28) and taking into account the comments made after Eq. (36), one can prove that

$$v_{m\varepsilon} \to v_m \quad \text{strongly in } H^2(0, \ell) \text{ as } \varepsilon \to 0, \tag{79}$$

$$\lim_{\varepsilon \to 0} \lambda_{m\varepsilon} = \lambda_m, \quad m = 1, 2, \ldots \ . \tag{80}$$

Here, $H^2(0, \ell)$ denotes the Hilbert space formed by the measurable functions $f, f : (0, \ell) \to \mathbb{R}$, such that both $f$ and its derivatives $f'$, $f''$ (in the sense of distributions) belong to $L^2(0, \ell)$. The second ingredient is the *fundamental identity*

$$(\lambda_{m\varepsilon} - \lambda_m) \int_0^\ell \rho(x) v_m v_{m\varepsilon} \,\mathrm{d}x = \int_0^\ell b_\varepsilon(x) v_m'' v_{m\varepsilon}'' \,\mathrm{d}x, \tag{81}$$

which holds for every $\varepsilon > 0$ and for every integer number $m$, $m = 1, 2, \ldots$ . Identity Eq. (81) follows by multiplying Eq. $(69)_1$ (with $(v_\varepsilon, \lambda_\varepsilon)$ replaced by the $m$th eigenpair $(v_{m\varepsilon}, \lambda_{m\varepsilon})$) by $v_m$ and Eq. $(75)_1$ (with $(v, \lambda)$ replaced by the $m$th eigenpair $(v_m, \lambda_m)$) by $v_{m\varepsilon}$, and by integration by parts. By Eqs. (79)–(81) the desired Taylor series expansion (77)–(78) follows. The above analysis can be clearly extended to consider beams with more general boundary conditions, see Section 5.2 for applications to free–free beams.

The integral term in the right-hand side of Eq. (77) shows that the sensitivity of the $m$th eigenvalue to variations of the bending stiffness depends on the square of the curvature of the $m$th vibration mode of the reference beam. The limit case of Eq. (77) for localized damages, as cracks or notches modelled by an elastic rotational spring inserted at the damaged cross-sections, was considered in Ref. [31].

The reconstruction procedure based on Eqs. (77)–(78) will be developed under the additional a priori assumption that the stiffness variation occurs on one half of the beam:

$$\text{supp } b_\varepsilon(x) \subset \left(0, \frac{\ell}{2}\right). \tag{82}$$

The case of an initially uniform beam will be firstly considered. The eigenpairs of the reference beam are given by

$$v_m(x) = \sqrt{\frac{2}{\rho \ell}} \sin \frac{m\pi x}{\ell}, \quad \lambda_m = \frac{j}{\rho} \left(\frac{m\pi}{\ell}\right)^4, \quad m = 1, 2, \ldots \ . \tag{83}$$

Inserting the expressions of $v_m$ and $\lambda_m$ into Eq. (81) gives

$$\lambda_{m\varepsilon} - \lambda_m = \left(\frac{m\pi}{\ell}\right)^4 \left(\frac{2}{\rho \ell}\right) \int_0^\ell b_\varepsilon(x) \sin^2 \frac{m\pi x}{\ell} \,\mathrm{d}x + r(\varepsilon, m), \quad m = 1, 2, \ldots, \tag{84}$$

where $r(\varepsilon, m)$ is an higher-order term on $\varepsilon$. Expressing $b_\varepsilon(x)$ in terms of the functions $\{\frac{(v_m'')^2}{\lambda_m}\}_{m=1}^\infty$, that is

$$b_\varepsilon(x) = \sum_{k=1}^\infty \beta_{\varepsilon k} \frac{(v_k'')^2}{\lambda_k} \tag{85}$$

and using the linearized form of Eq. (84), one has

$$\delta\lambda_{m\varepsilon} = \sum_{k=1}^{\infty} A_{mk}\beta_{\varepsilon k}, \quad m = 1, 2, \ldots, \tag{86}$$

where

$$\delta\lambda_{m\varepsilon} \equiv \frac{\lambda_{m\varepsilon} - \lambda_m}{\lambda_m}, \quad m = 1, 2, \ldots \ . \tag{87}$$

If, as it was made for the axial vibration case, only the first $M$ eigenfrequencies are considered as data in identification, then the $M$-approximation $\beta_{\varepsilon k}^M$ of $\beta_{\varepsilon k}$, see Section 3, has the explicit expression (50) and, finally, the first-order approximation of the bending stiffness variation is given by

$$b_\varepsilon(x) = 8j \sum_{k=1}^{M} \left( \frac{2M-1}{2M+1}\delta\lambda_{k\varepsilon} - \frac{2}{2M+1} \sum_{j=1, j\neq k}^{M} \delta\lambda_{j\varepsilon} \right) \sin^2 \frac{k\pi x}{\ell}. \tag{88}$$

This completes the study of the linearized inverse problem. The analysis of the general case is based on iterative application of the above linearized approach. The main steps of the numerical algorithm are essentially those already explained in Section 3 for the longitudinal vibration case. The numerical code is based on a finite element model of the beam with uniform mesh and cubic displacement shape functions. The stiffness and mass coefficients are approximated with constant value functions within the generic $e$th finite element. The local consistent-mass (for translational inertia) and the stiffness matrices are given by

$$M_e = \frac{\rho_e \Delta}{420} \begin{pmatrix} 156 & 22\Delta & 54 & -13\Delta \\ 22\Delta & 4\Delta^2 & 13\Delta & -3\Delta^2 \\ 54 & 13\Delta & 156 & -22\Delta \\ -13\Delta & -3\Delta^2 & -22\Delta & 4\Delta^2 \end{pmatrix}, \tag{89}$$

$$K_e = \frac{j_e}{\Delta^3} \begin{pmatrix} 12 & 6\Delta & -12 & 6\Delta \\ 6\Delta & 4\Delta^2 & -6\Delta & 2\Delta^2 \\ -12 & -6\Delta & 12 & -6\Delta \\ 6\Delta & 2\Delta^2 & -6\Delta & 4\Delta^2 \end{pmatrix}, \tag{90}$$

where $\Delta$ is the length of the generic element. The second derivative of the eigenfunctions was estimated by using a finite difference approximation on the rotational degrees of freedom of the discrete finite element model.

### 5.2. Applications

The above reconstruction technique was tested to detect damage on several real beams in bending vibration. The results obtained on a free–free beam with solid square cross-section, beam 1 of Fig. 12, are briefly summarized in the sequel. The beam is studied under free–free boundary conditions and the finite element model includes 100 equally spaced finite elements. With this fine mesh, the first lower frequencies of the discrete model are practically indistinguishable from those of the Euler–Bernoulli model.

The specimen was suspended from above by means of two soft springs, so to simulate free–free boundary conditions. It should be recalled that the free–free beam has a double multiplicity zero eigenvalue, corresponding to two independent rigid body motions. These vibrating modes are insensitive to damage and will be omitted in the sequel. The damage consisted of two symmetric notches placed at the cross-section at 0.255 m from the left end, see Fig. 12. Their depth was progressively increased by 1 mm at a time from the undamaged configuration to a final level of damage $D6$ corresponding to a depth of 6 mm on both sides of the cross-section. For each level, the lowest seven natural frequencies were measured according to an *impulse*

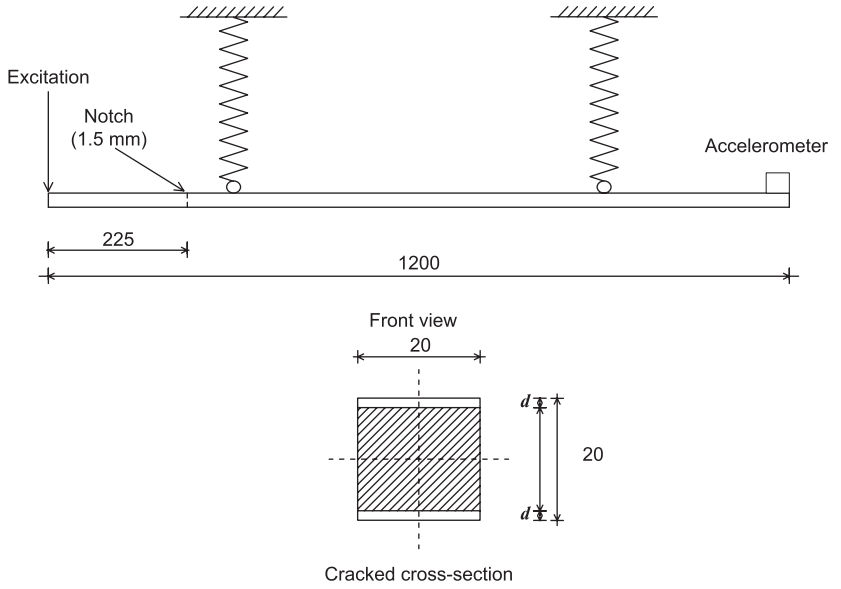


Fig. 12. Experimental model of bending vibrating beam (beam 1) and damage configurations. Lengths in mm.

Table 4
Experimental frequencies of beam 1 and analytical values for the undamaged configuration (rigid body motions are omitted)

| Mode | Undamaged | | | $D1$ | | $D2$ | | $D3$ | | $D4$ | | $D5$ | | $D6$ | |
|---|---|---|---|---|---|---|---|---|---|---|---|---|---|---|---|
| $n$ | Exper. | Model | $\Delta_n\%$ | Exper. | $\Delta_n\%$ | Exper. | $\Delta_n\%$ | Exper. | $\Delta_n\%$ | Exper. | $\Delta_n\%$ | Exper. | $\Delta_n\%$ | Exper. | $\Delta_n\%$ |
| 1 | 72.19 | 72.19 | 0.00 | 72.19 | 0.00 | 72.16 | −0.05 | 72.16 | −0.05 | 72.06 | −0.18 | 71.94 | −0.35 | 71.53 | −0.91 |
| 2 | 198.40 | 198.99 | 0.30 | 198.31 | −0.04 | 198.06 | −0.17 | 197.68 | −0.36 | 196.44 | −0.99 | 194.69 | −1.87 | 189.25 | −4.61 |
| 3 | 387.73 | 390.11 | 0.61 | 387.50 | −0.06 | 386.84 | −0.23 | 385.33 | −0.62 | 381.56 | −1.59 | 374.97 | −3.29 | 360.96 | −6.90 |
| 4 | 639.72 | 644.87 | 0.81 | 639.38 | −0.05 | 638.41 | −0.21 | 636.28 | −0.54 | 630.81 | −1.39 | 623.78 | −2.49 | 607.03 | −5.11 |
| 5 | 951.47 | 963.33 | 1.25 | 951.31 | −0.02 | 950.75 | −0.08 | 950.03 | −0.15 | 947.03 | −0.47 | 943.47 | −0.84 | 935.16 | −1.71 |
| 6 | 1320.56 | 1345.47 | 1.89 | 1320.56 | 0.00 | 1320.34 | −0.02 | 1320.25 | −0.02 | 1319.97 | −0.04 | 1319.97 | −0.04 | 1319.16 | −0.11 |
| 7 | 1747.03 | 1791.30 | 2.53 | 1746.81 | −0.01 | 1746.63 | −0.02 | 1746.13 | −0.05 | 1742.88 | −0.24 | 1739.41 | −0.44 | 1728.28 | −1.07 |

Undamaged configuration: $EJ = 2627.32\,\mathrm{Nm}^2$, $\rho = 3.083\,\mathrm{kg/m}$, $\ell = 1.200\,\mathrm{m}$; $\Delta_n\% = 100 \cdot (f_n^{\mathrm{model}} - f_n^{\mathrm{exp}})/f_n^{\mathrm{exp}}$. Damage scenarios $D1$–$D6$; abscissa of the cracked cross-section: $s = 0.225\,\mathrm{m}$; $\Delta_n\% = 100 \cdot (f_n^{\mathrm{dam}} - f_n^{\mathrm{undam}})/f_n^{\mathrm{undam}}$. Frequency values in Hz.

*technique*, see Ref. [4] for more details on the experiments. Beam 1 provides an example for which the analytical Euler–Bernoulli model is fairly good in the full range of measured frequencies, with percentage deviations which are less than 3% on the range of frequency of interest, cf. Table 4. However, frequency variations between the undamaged and damaged configurations are very small so that, at least up to the fourth level of damage $D4$, they become mixed up with the modelling errors. In fact, the identification gives poor results up to damage level $D4$, see Figs. 13–15. It is worth noting that the use of frequencies $f_5$–$f_7$ that are affected by relatively large model errors, as compared with the frequency changes induced by the damage, leads to unsatisfactory stiffness distribution. Starting from level $D5$, a clear tendency emerges to a reduction of stiffness localized around the real position of the damage. Again it can be shown that use of higher frequencies such as $f_6$ and $f_7$ obscures this trend until the damage becomes particularly severe.

## 6. A comparison with a variational-type method

In this section, an identification technique based on a variational-type method will be presented and applied to damage detection in beams. The results will be compared with those obtained by the Fourier coefficient procedure illustrated in the previous sections.

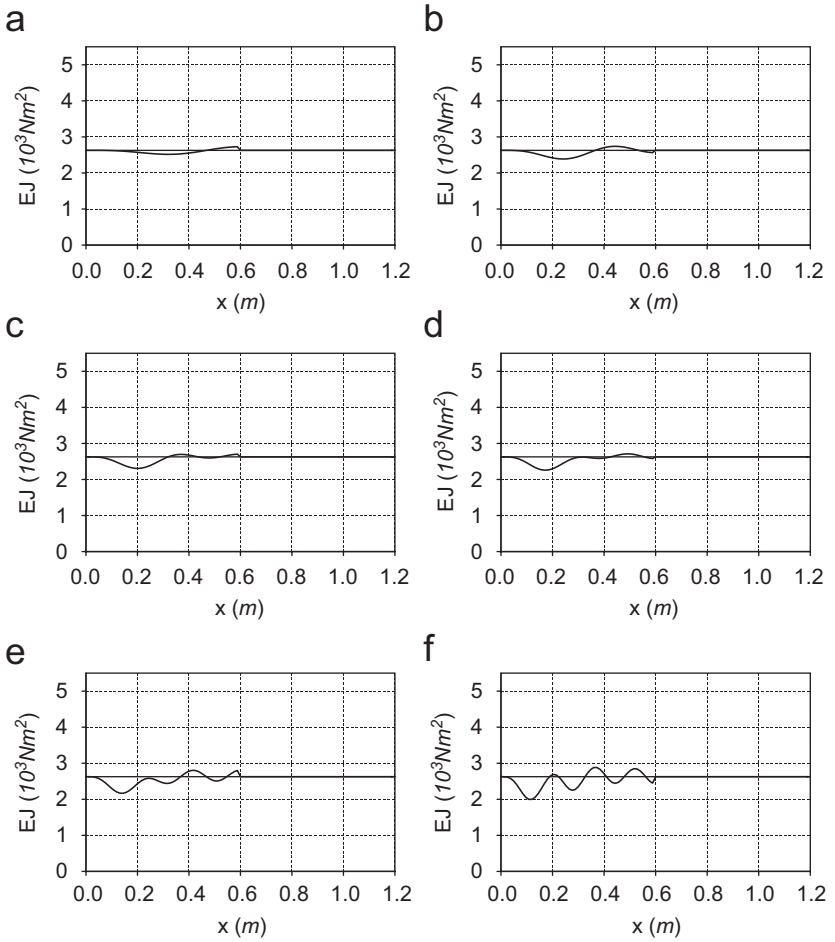


Fig. 13. (a)–(f) Beam 1: identified bending stiffness $EJ$ for damage $D3$ with $M = 2$ (a), $M = 3$ (b), $M = 4$ (c), $M = 5$ (d), $M = 6$ (e) and $M = 7$ (f) frequencies. Actual damage location $s = 0.225$ m.

The literature of variational-type methods based on eigenfrequency data is extensive, see, for example, the book [2] for a general overview and Refs. [1,8–16,28] for specific applications. Here, reference is made to the procedure adopted in Refs. [3,4] in the study of cracked beams by means of discrete models based on a special lumping of the stiffness and inertial properties of the continuous systems, and then extended in Ref. [18] to standard finite element models of beam structures.

Following is an outline of the identification technique in the case of a continuous Euler–Bernoulli beam in free bending vibration. The continuous model of the beam is substituted by a $N$ degree of freedom finite element model, whose free undamped vibrations are governed by the discrete eigenvalue problem

$$\mathbf{K}^N \mathbf{v}_n^N = \lambda_n^N \mathbf{M}^N \mathbf{v}_n^N, \tag{91}$$

where $\lambda_n^N \equiv (2\pi f_n^N)^2$ and $\mathbf{v}_n^N$, $\mathbf{v}_n^N \neq \mathbf{0}, n = 1, \ldots, N$, are the eigenvalues and eigenvectors of the discrete system, respectively. As usual, the global stiffness matrix $\mathbf{K}^N$ and the global mass matrix $\mathbf{M}^N$ are obtained by assembling the contribution of all the $N$ elements of the discrete model. In particular

$$\mathbf{K}^N = \sum_{e=1}^{N} \alpha_e \mathbf{K}_e, \tag{92}$$

where $\mathbf{K}_e$ is the stiffness matrix of the $e$th finite element and $\{\alpha_e\}_{e=1}^N$ is the collection of the "stiffness multipliers", see expression (90).

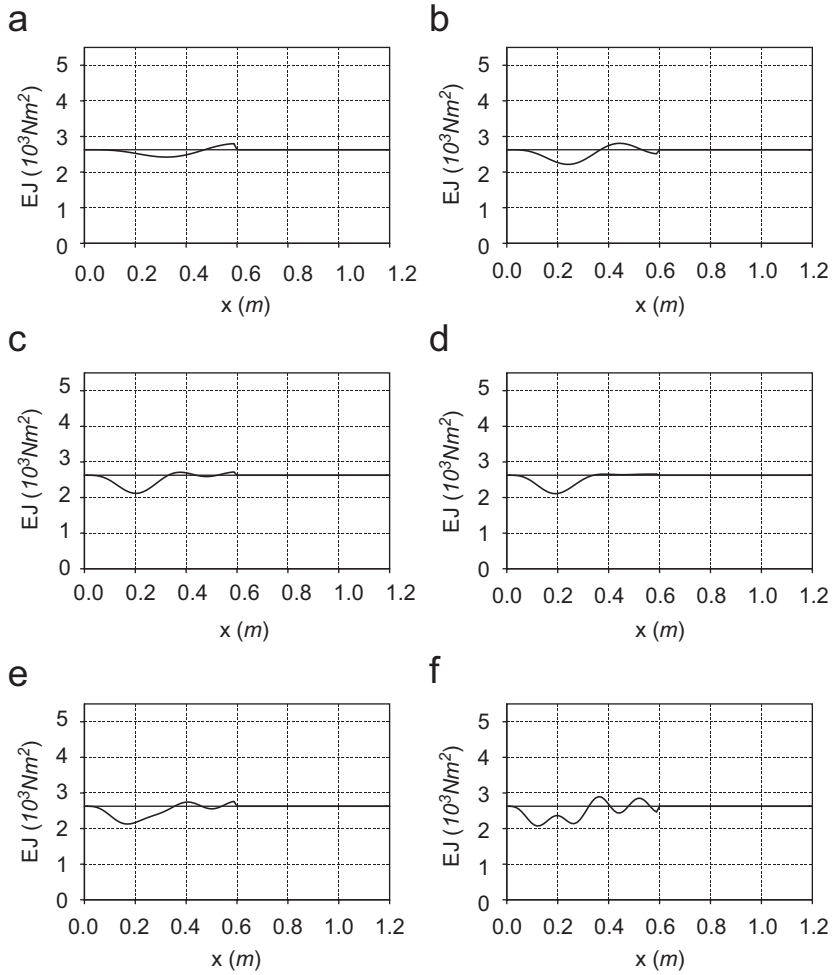


Fig. 14. (a)–(f) Beam 1: identified bending stiffness $EJ$ for damage $D4$ with $M = 2$ (a), $M = 3$ (b), $M = 4$ (c), $M = 5$ (d), $M = 6$ (e) and $M = 7$ (f) frequencies. Actual damage location $s = 0.225$ m.

It is assumed that the presence of a concentrate damage can be described within the framework of Euler–Bernoulli theory of beams and that it reflects into a localized reduction of the effective bending stiffness or, equivalently, a reduction of the multiplier $\alpha_e$ in the whole finite element. Then, one can consider the collection of $\alpha_e$s as descriptive of the stiffness distribution for the damaged system.

The approach to identification is of variational type and the problem becomes the following:

$$\text{to find } \{\alpha_e^{\text{opt}}\}_{e=1}^{P} \in \mathbb{R}^P \text{ such that } F(\alpha_1^{\text{opt}}, \ldots, \alpha_P^{\text{opt}}) = \min F(\alpha_1, \ldots, \alpha_P) \tag{93}$$

for $\alpha_e > 0$, $e = 1, \ldots, P$, where the distance between the first $M$ experimental $\lambda_n^{\text{exp}}$ and analytical $\lambda_n^{\text{model}}$ eigenvalues is given by

$$F(\alpha_1, \ldots, \alpha_P) = \sum_{n=1}^{M} \left( 1 - \frac{\lambda_n^{\text{model}}(\alpha_1, \ldots, \alpha_P)}{\lambda_n^{\text{exp}}} \right)^2. \tag{94}$$

An iterative algorithm based on an optimal gradient descent method has been used in solving the minimization problem (93)–(94), see Ref. [3] for more details. Since the variational problem is not convex, the success of the technique crucially depends on the choice of a good initial estimate of the stiffness multipliers to be identified. Here, the stiffness distribution of the undamaged beam has been chosen as initial point in

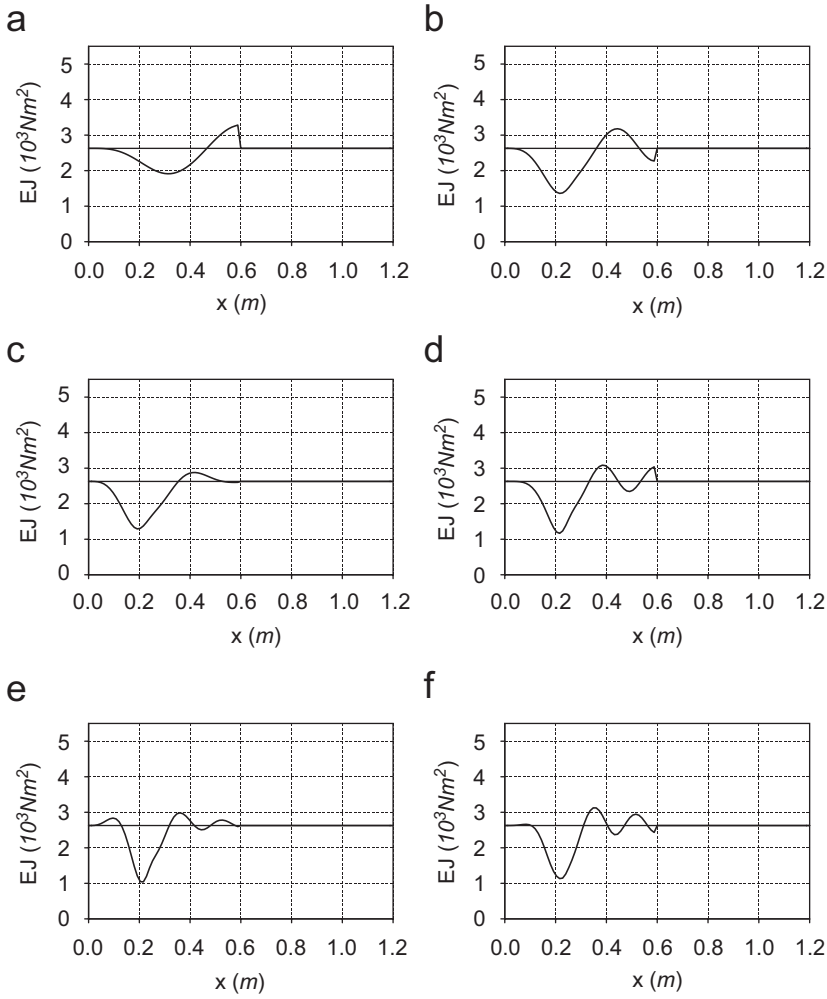


Fig. 15. (a)–(f) Beam 1: identified bending stiffness $EJ$ for damage $D6$ with $M = 2$ (a), $M = 3$ (b), $M = 4$ (c), $M = 5$ (d), $M = 6$ (e) and $M = 7$ (f) frequencies. Actual damage location $s = 0.225$ m.

minimization. Finally, the iterations go on until the relative variation of $F(\alpha_e) \equiv F(\alpha_1, \ldots, \alpha_P)$ and $\{\alpha_1, \ldots, \alpha_P\}$ at the $k$th step satisfy a chosen criterion of smallness, namely

$$\left|\frac{F(\alpha_e^{(k+1)}) - F(\alpha_e^{(k)})}{F(\alpha_e^{(k)})}\right| + \sum_{e=1}^{P}\left|\frac{\alpha_e^{(k+1)} - \alpha_e^{(k)}}{\alpha_e^{(k)}}\right| \leqslant 10^{-6}. \tag{95}$$

The variational method has been applied for damage identification in the same experimental models presented in Section 4 (axial vibrating rods) and in Section 5.2 (bending vibration beams). In particular, the results obtained on a free–free bending vibrating beam with solid square section of Fig. 12 (beam 1 of Section 5.2) are discussed in detail in the sequel. The finite element model includes 100 equally spaced finite elements and, as before, the damage is supposed to occur on the left half of the beam.

The results of identification are summarized in Figs. 16–18 for damage $D3$, $D4$ and $D6$, respectively. It turns out that the optimal stiffness distributions obtained by solving the variational problem (93)–(94) are very close to those deduced by the *Fourier coefficient method* (see Figs. 13–15). Similar results have been obtained in studying all the other experimental models (rods 1, 2 and 3 of Section 4).

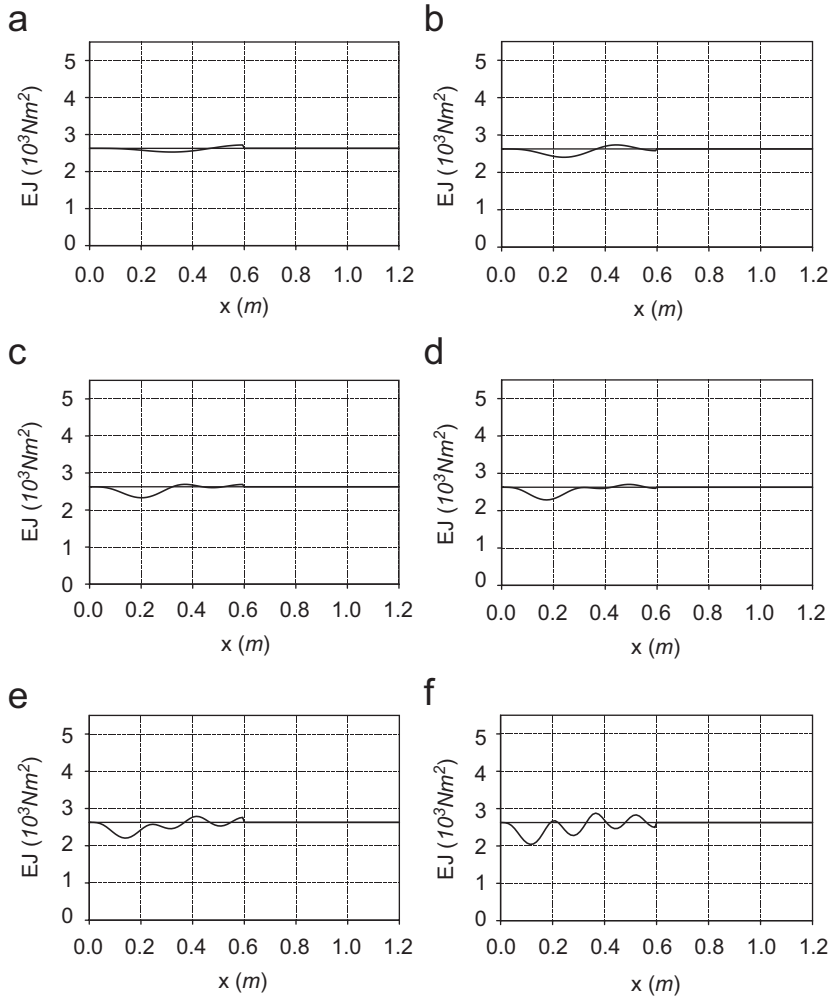


Fig. 16. (a)–(f) Beam 1 (optimization method): identified bending stiffness $EJ$ for damage $D3$ with $M = 2$ (a), $M = 3$ (b), $M = 4$ (c), $M = 5$ (d), $M = 6$ (e) and $M = 7$ (f) frequencies. Actual damage location $s = 0.225$ m.

## 7. Concluding remarks

The first part of this paper has been focussed on detecting damage from the knowledge of the damage-induced shifts in lower frequencies of a longitudinally vibrating rod under free–free boundary conditions. Under the a priori assumption that the damage belongs to a half of the rod and the linear mass density remains unchanged, it was shown that frequency shifts can be used to determine certain generalized Fourier coefficients of the axial stiffness variation caused by the damage. From a general point of view, this diagnostic problem is a version of the Hochstadt–Lieberman result proved in Ref. [46] when only finite eigenvalue data is available. More precisely, on adapting the arguments of Ref. [46], it can be shown that if the axial stiffness of a longitudinally vibrating rod is known on a half of the rod, then the full set of natural frequencies determines uniquely the axial stiffness on the remaining half of the rod. Unfortunately, it is not know, to the best of the author knowledge, a corresponding stability result when only the first lower eigenvalues are available. Nevertheless, the proposed diagnostic technique provided a satisfactory identification of the damage, both for position and severity, when the first 5–10 eigenvalues are considered in the analysis and frequency shifts induced by the damage are bigger than modelling and measurement errors.

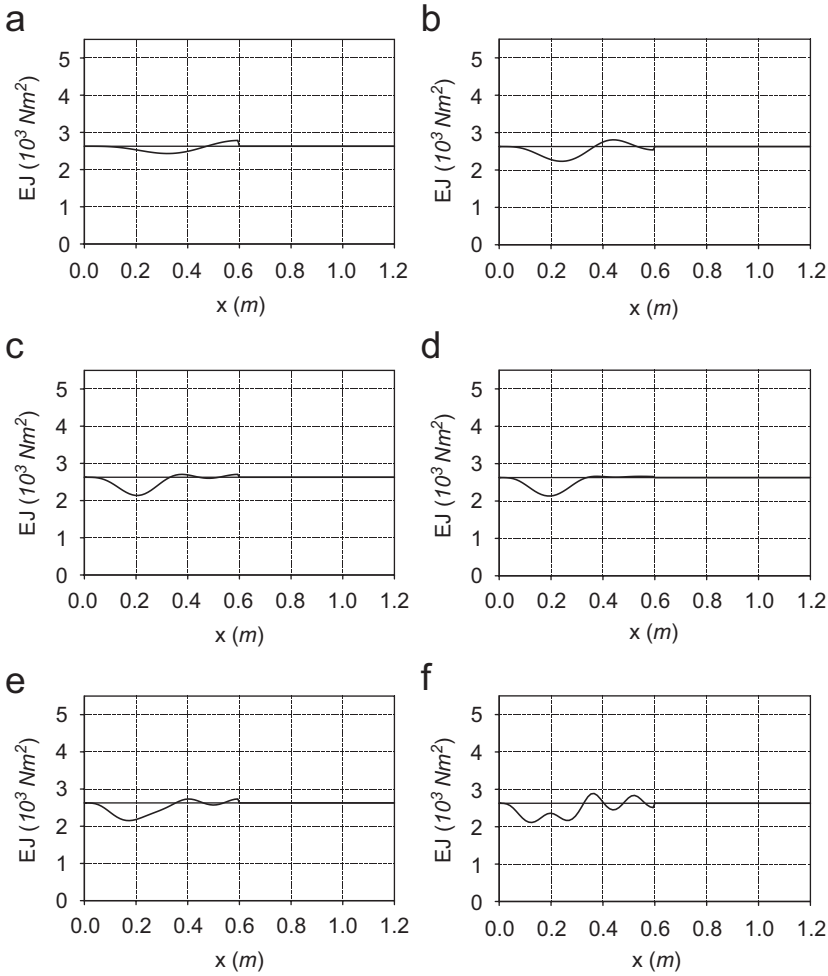


Fig. 17. (a)–(f) Beam 1 (optimization method): identified bending stiffness $EJ$ for damage $D4$ with $M = 2$ (a), $M = 3$ (b), $M = 4$ (c), $M = 5$ (d), $M = 6$ (e) and $M = 7$ (f) frequencies. Actual damage location $s = 0.225$ m.

The second part of the paper has been devoted to the study of the corresponding diagnostic problem for pinned–pinned beams in transversal vibration. As before, the bending stiffness is given on a half of the beam and the frequency shifts induced by the damage on first lower frequencies are used to reconstruct the stiffness on the remaining half of the beam and, finally, to identify position and severity of the damage. For the corresponding mathematical inverse problem, a result analogous to that proved by Hochstadt and Lieberman in [46] is not available, see Refs. [47–51] for recent contributions concerning the Euler–Bernoulli model. However, despite there is no proof of uniqueness of the reconstruction, applications of proposed technique to steel beams with localized damages gave results that can be considered satisfactory from the practical point of view.

Finally, the results of damage identification obtained via *Fourier coefficient method* and by using a standard variational method based on frequency data for all the experimental models, both under axial or bending vibrations, have been compared. The comparison shows a good agreement between the outcome of the two methods in all the cases studied. This leads to the conjecture that, at least in simple beam models, updating the stiffness distribution so that the distance between the first $M$ measured and analytical frequencies is minimized, is equivalent to finding the first $M$ generalized Fourier coefficients of the stiffness variation caused by the damage.

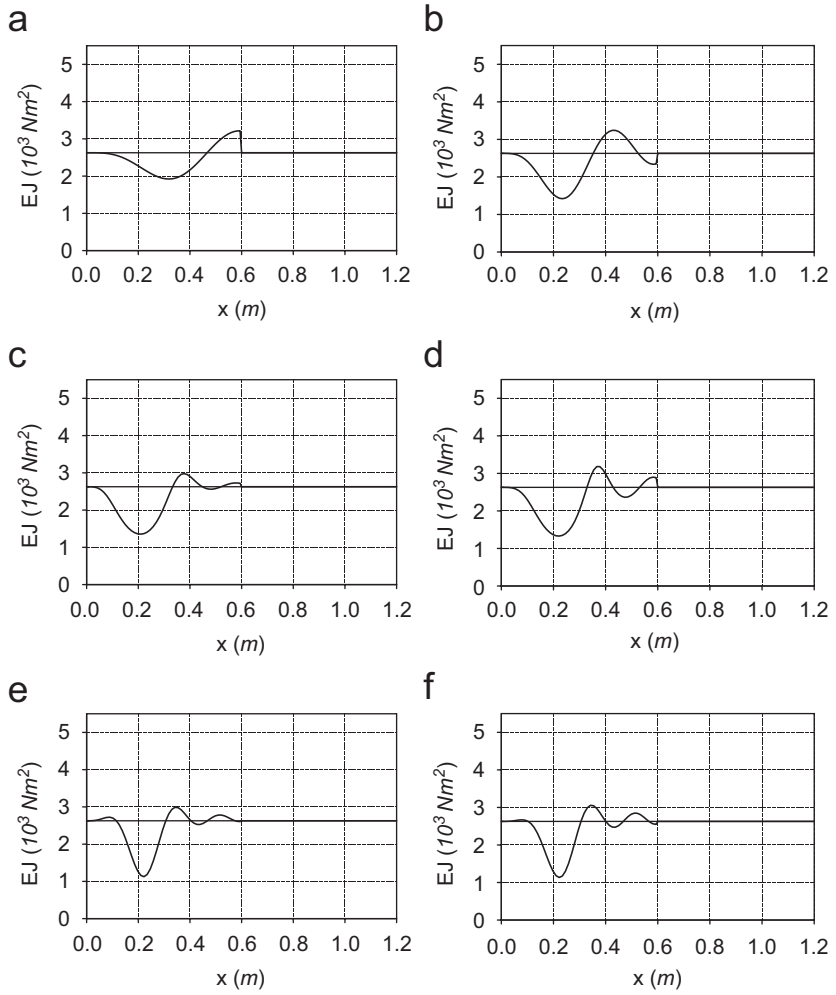


Fig. 18. (a)–(f) Beam 1 (optimization method): identified bending stiffness $EJ$ for damage $D6$ with $M = 2$ (a), $M = 3$ (b), $M = 4$ (c), $M = 5$ (d), $M = 6$ (e) and $M = 7$ (f) frequencies. Actual damage location $s = 0.225$ m.

As it emerges from the above considerations, there are several open problems associated with the proposed diagnostic technique. Firstly, the convergence of the iterative procedure. Secondly, the connection with general results of the inverse eigenvalue theory. Thirdly, the relationship between the Fourier coefficient method and variational methods based on frequency measurements. All these problems require further investigation.

## References

[1] R.D. Adams, P. Cawley, C.J. Pye, B.J. Stone, A vibration technique for non-destructively assessing the integrity of structures, *Journal of Mechanical Engineering Science* 20 (2) (1978) 93–100.
[2] M.I. Friswell, J.E. Mottershead, *Finite Element Model Updating in Structural Dynamics*, Kluwer Academic Publishers, Dordrecht, 1995.
[3] C. Davini, F. Gatti, A. Morassi, A damage analysis of steel beams, *Meccanica* 28 (1993) 27–37.
[4] C. Davini, A. Morassi, N. Rovere, Modal analysis of notched bars: tests and comments on the sensitivity of an identification technique, *Journal of Sound and Vibration* 179 (3) (1995) 513–527.
[5] G.M.L. Gladwell, *Inverse Problems in Vibration*, Martinus Nijhoff Publishers, Dordrecht, 1986.
[6] G.M.L. Gladwell, *Inverse Problems in Vibration*, second ed., Kluwer Academic Publishers, Dordrecht, 2004.

[7] T.G. Chondros, A.D. Dimarogonas, Identification of cracks in welded joints of complex structures, *Journal of Sound and Vibration* 69 (4) (1980) 531–538.
[8] R.Y. Liang, J. Hu, F. Choy, Quantitative NDE technique for assessing damages in beam structures, *ASCE Journal of Engineering Mechanics* 118 (7) (1992) 1468–1487.
[9] M.N. Cerri, F. Vestroni, Detection of damage in beams subjected to diffused cracking, *Journal of Sound and Vibration* 234 (2) (2000) 259–276.
[10] F. Vestroni, D. Capecchi, Damage detection in beam structures based on frequency measurements, *ASCE Journal of Engineering Mechanics* 126 (2000) 761–768.
[11] P. Hajela, F.J. Soeiro, Structural damage detection based on static and modal analysis, *AIAA Journal* 28 (6) (1990) 1110–1115.
[12] G. Hearn, R.B. Testa, Modal analysis for damage detection in structures, *ASCE Journal of Structural Engineering* 117 (1991) 3042–3063.
[13] S. Hassiotis, G.D. Jeong, Assessment of structural damage from natural frequency measurements, *Computer & Structures* 49 (4) (1993) 679–691.
[14] S.S. Law, Z.Y. Shi, L.M. Zhang, Structural damage detection from incomplete and noisy modal test data, *ASCE Journal of Engineering Mechanics* 124 (11) (1998) 1280–1288.
[15] J.B. Kosmatka, J.M. Ricles, Damage detection in structures by modal vibration characterization, *ASCE Journal of Structural Engineering* 125 (12) (1999) 1384–1392.
[16] D. Capecchi, F. Vestroni, Monitoring of structural systems by using frequency data, *Earthquake Engineering and Structural Dynamics* 28 (2000) 447–461.
[17] W.X. Ren, G. De Roeck, Structural damage identification using modal data, I: simulation verification, *ASCE Journal of Structural Engineering* 128 (1) (2002) 87–95.
[18] A. Morassi, N. Rovere, Localizing a notch in a steel frame from frequency measurements, *ASCE Journal of Engineering Mechanics* 123 (5) (1997) 422–432.
[19] G. Borg, Eine Umkehrung der Sturm–Liouvilleschen Eigenwertaufgabe: Bestimmung der Differentialgleichung durch die Eigenwerte, *Acta Mathematica* 78 (1946) 1–96.
[20] O. Hald, The inverse Sturm–Liouville problem and the Rayleigh–Ritz method, *Mathematics of Computation* 32 (143) (1978) 687–705.
[21] R. Knobel, B.D. Lowe, An inverse Sturm–Liouville problem for an impedance, *Zeitschrift fur Angewandte Mathematik Und Physik* 44 (1993) 433–450.
[22] Q. Wu, Reconstruction of integrated crack function of beams from eigenvalue shifts, *Journal of Sound and Vibration* 173 (2) (1994) 279–282.
[23] Q. Wu, F. Fricke, Determination of blocking locations and cross-sectional area in a duct by eigenfrequency shifts, *Acoustical Society of America* 87 (1) (1990) 67–75.
[24] H.F. Weinberger, *A First Course in Partial Differential Equations*, Dover Publications Inc., New York, 1965.
[25] W.T. Thomson, Vibration of slender bars with discontinuities in stiffness, *Journal of Applied Mechanics* 16 (1949) 203–207.
[26] H.J. Petroski, Comments on "Free vibration of beams with abrupt changes in cross-section", *Journal of Sound and Vibration* 92 (1) (1984) 157–159.
[27] S. Christidies, A.D.S. Barr, One-dimensional theory of cracked Bernoulli–Euler beams, *International Journal of the Mechanical Science* 26 (11/12) (1984) 639–648.
[28] J.K. Sinha, M.I. Friswell, S. Edwards, Simplified models for the location of cracks in beam structures using measured vibration data, *Journal of Sound and Vibration* 251 (1) (2002) 13–38.
[29] H. Brezis. *Analisi Funzionale*, Liguore Editore, Napoli, 1986.
[30] P. Gudmundson, Eigenfrequency changes of structures due to cracks, notches or other geometrical changes, *Journal of Mechanics and Physics of Solids* 30 (5) (1982) 339–353.
[31] A. Morassi, Crack-induced changes in eigenparameters of beam structures, *ASCE Journal of Engineering Mechanics* 119 (9) (1993) 1798–1803.
[32] Y. Narkis, Identification of crack location in vibrating simply supported beams, *Journal of Sound and Vibration* 172 (1994) 549–558.
[33] A. Morassi, Identification of a crack in a rod based on changes in a pair of natural frequencies, *Journal of Sound and Vibration* 242 (2001) 577–596.
[34] A. Morassi, M. Rollo, Identification of two cracks in a simply supported beam from minimal frequency measurements, *Journal of Vibration and Control* 7 (2001) 729–739.
[35] S.P. Lele, S.K. Maiti, Modelling of transverse vibration of short beams for crack detection and measurement of crack extension, *Journal of Sound and Vibration* 257 (3) (2002) 559–583.
[36] M. Dilena, A. Morassi, Damage detection in discrete vibrating systems, *Journal of Sound and Vibration* 289 (4–5) (2006) 830–850.
[37] M.M.F. Yuen, A numerical study of the eigenparameters of a damaged cantilever, *Journal of Sound and Vibration* 103 (3) (1985) 301–310.
[38] P.F. Rizos, N. Aspragathos, A.D. Dimarogonas, Identification of crack location and magnitude in a cantilever beam from the vibration modes, *Journal of Sound and Vibration* 138 (3) (1990) 381–388.
[39] A.K. Pandey, M. Biswas, M.M. Samman, Damage detection from changes in curvature mode shapes, *Journal of Sound and Vibration* 145 (2) (1991) 321–332.
[40] G.M.L. Gladwell, A. Morassi, Estimating damage in a rod from changes in node positions, *Inverse Problems in Engineering* 7 (3) (1999) 215–233.

[41] M. Dilena, A. Morassi, Identification of crack location in vibrating beams from changes in node positions, *Journal of Sound and Vibration* 255 (5) (2002) 915–930.
[42] M. Dilena, A. Morassi, The use of antiresonances for crack detection in beams, *Journal of Sound and Vibration* 276 (1–2) (2004) 195–214.
[43] R.W. Clough, J. Penzien, *Dynamics of Structures*, McGraw-Hill International Publishers, Singapore, 1975.
[44] G. Borg, On the completeness of some sets of functions, *Acta Mathematica* 81 (1949) 265–283.
[45] A. Morassi, A uniqueness result on crack location in vibrating rods, *Inverse Problems in Engineering* 4 (1997) 231–254.
[46] H. Hochstadt, B. Lieberman, An inverse Sturm–Liouville problem with mixed given data, *SIAM Journal of Applied Mathematics* 34 (4) (1978) 676–680.
[47] D.C. Barnes, The inverse eigenvalue problem with finite data, *SIAM Journal of Mathematical Analysis* 22 (3) (1991) 732–753.
[48] B.D. Lowe, On the construction of an Euler–Bernoulli beam from spectral data, *Journal of Sound and Vibration* 163 (1) (1993) 165–171.
[49] A. Elcrat, V.G. Papanicolau, On the inverse problem of a fourth-order self-adjoint binomial operator, *SIAM Journal of Mathematical Analysis* 28 (4) (1997) 886–896.
[50] L.F. Caudill, P.A. Perry, A.W. Schueller, Isospectral sets for fourth-order ordinary differential operators, *SIAM Journal of Mathematical Analysis* 29 (4) (1998) 935–966.
[51] A. Schueller, Uniqueness for near-constant data in fourth-order inverse eigenvalue problems, *Journal of Mathematical Analysis and Applications* 258 (2001) 658–670.